AD_____

Award Number: W81XWH-10-1-0751

TITLE: Oxygenation-Enhanced Radiation Therapy of Breast Tumors

PRINCIPAL INVESTIGATOR: Dr. Mikhail Skliar

CONTRACTING ORGANIZATION: The University of Utah
Salt Lake City, UT 84112

REPORT DATE: November 2011

TYPE OF REPORT: Final

PREPARED FOR: U.S. Army Medical Research and Materiel Command
Fort Detrick, Maryland 21702-5012

DISTRIBUTION STATEMENT: Approved for public release; distribution unlimited

REPORT DOCUMENTATION PAGE

Form Approved
OMB No. 0704-0188

1. REPORT DATE *(DD-MM-YYYY)*	**2. REPORT TYPE**	**3. DATES COVERED** *(From - To)*
01-11-2011	Final	1 SEP 2010 - 31 Oct 2011

4. TITLE AND SUBTITLE
Oxygenation-Enhanced Radiation Therapy of Breast Tumors

5a. CONTRACT NUMBER

5b. GRANT NUMBER
W81XWH-10-1-0751

5c. PROGRAM ELEMENT NUMBER

6. AUTHOR(S)
Dr. Mikhail Skliar

E-Mail: mikhail.skliar@utah.edu

5d. PROJECT NUMBER

5e. TASK NUMBER

5f. WORK UNIT NUMBER

7. PERFORMING ORGANIZATION NAME(S) AND ADDRESS(ES)
The University of Utah
Salt Lake City, UT 84112

8. PERFORMING ORGANIZATION REPORT NUMBER

9. SPONSORING / MONITORING AGENCY NAME(S) AND ADDRESS(ES)
U.S. Army Medical Research and Materiel Command
Fort Detrick, Maryland 21702-5012

10. SPONSOR/MONITOR'S ACRONYM(S)

11. SPONSOR/MONITOR'S REPORT NUMBER(S)

12. DISTRIBUTION / AVAILABILITY STATEMENT
Approved for Public Release; Distribution Unlimited

13. SUPPLEMENTARY NOTES

14. ABSTRACT
The treatment of locoregional breast cancer has evolved from radical mastectomy to targeted local therapy with breast conservation. The efficacy of conserving treatments of breast cancers is impeded by tumor hypoxia, which affects 50% of locally advanced breast tumors. Poor oxygenation of hypoxic tumors reduces their sensitivity to X-ray and γ-radiation, which requires a high radiation dose for efficacy compared to normally oxygenated tissues. This Concept project provides initial investigation the method for targeted oxygen release from oxygen carriers as a step towards as a novel strategy of radio sensitization of hypoxic breast tumors, and studies the effect of different targeting mechanisms on the oxygen mass transfer. Specific results include the development of stabilized perfluorocarbon emulsions as oxygen carriers, their characterization, and response to external triggers, including elevated temperature, reduced pressure, and dwell time.

15. SUBJECT TERMS
Targeted oxygenation, perfluorocarbon emulsions, breast cancer

16. SECURITY CLASSIFICATION OF:			**17. LIMITATION OF ABSTRACT**	**18. NUMBER OF PAGES**	**19a. NAME OF RESPONSIBLE PERSON**
a. REPORT	**b. ABSTRACT**	**c. THIS PAGE**			USAMRMC
U	U	U	UU	29	**19b. TELEPHONE NUMBER** *(include area code)*

Table of Contents

Introduction

The treatment of locoregional breast cancer has evolved from radical mastectomy to targeted local therapy with breast conservation. The efficacy of conserving treatments of breast cancers is impeded by tumor hypoxia. It has been reported [1] that close to 50% of locally advanced breast cancers exhibit hypoxic or even anoxic regions within a tumor mass. Poor oxygenation of hypoxic tumors reduces their sensitivity to X-ray and γ-radiation, which requires a high radiation dose for efficacy compared to normally oxygenated tissues [2]. This increase is approximately 3-fold in the case of X-ray therapy [3], which limits re-treatment options. This Concept Grant performed initial investigation of the proposed novel strategy of radio sensitization of hypoxic breast tumors by targeted oxygen release from perfluorocarbon oxygen carriers. In the proposed approach, an emulsion of oxygen-saturated perfluorocarbon droplets, less than 5μm in diameter and as small as 100nm, was stabilized by a biocompatible amphiphilic block co-polymer, PEG-PLLA. Though perfluorocarbon (PFC) emulsions have been studied for a long time as potential blood oxygen careers and are currently approved for limited use during heart surgery [4], the key difference of the proposed approach compared to the previously investigated use of PEG conjugated hemoglobin as an oxygenation adjuvant to radiation therapy [5] is the potential for active targeting and control of the O2 release at the tumor site. This report summarizes our initial finding on the proposed method, including the method to produce the oxygen carriers, characterization of their properties, and the response to an external excitation, such as elevated temperature, reduced pressure, and radiation.

Body

We hypothesized that the preferential release of oxygen from PFC droplets inside or in the proximity of the tumor can be achieved by targeted, localized heating, sonication, and radiation. Because O2 solubility in PFC is substantially higher than in blood, oxygen release from PFC droplets is not thermodynamically favored. When it does occur, the release location cannot be controlled, as in the case of oxygenation with PEG conjugated Hb. We hypothesize that the phase transition of PFC droplets to bubbles will increase the oxygen fugacity and favor the transfer of oxygen into the blood stream. In order to cause phase transition, PFC inside the droplets must be supersaturated. The supersaturation can be achieved by lowering pressure or increasing temperature. Targeted (focused) ultrasound (US) can be used to selectively heat the target. Other heating modalities (non-invasive & invasive) are available and commonly used in hyperthermia and ablative therapies. In addition to thermal effects, the US transiently lowers the pressure which also favors bubble formation.

Our investigation started with the development of the method for creating the stabilized perfluoropentane (PFP) emulsions intended as the oxygen carrier system.

Task 1. Preparation of PFP emulsions

Stable microdroplets of PFP are formed using stabilizing surfactant coatings. Primarily, poly (ethylene glycol) – co – poly (L-Lactide) (PEG-PLLA) were used by us as a stabilizing agent. Structures of PFP and PEG-PLLA are shown in Figure 1. Most results were obtained using the molecular weight of the block copolymers of 5000 Da and 4700 for PEG and PLLA respectively.

PEG-PLLA is known to form micelles at critical micellar concentration (CMC) of 0.0071-0.0092 mM [6]. We characterized the size distribution of micelles for different concentrations of the surfactant by dynamic light scattering. Size distributions were obtained at room temperature for different polymer concentrations. Figure 2a shows distinct peaks, with the population of smaller micelles centered at approximately 20 nm and larger micelles at ~85 nm. As the concentration of PEG-PLLA decreases, the size distributions of micelles shifts toward lower values.

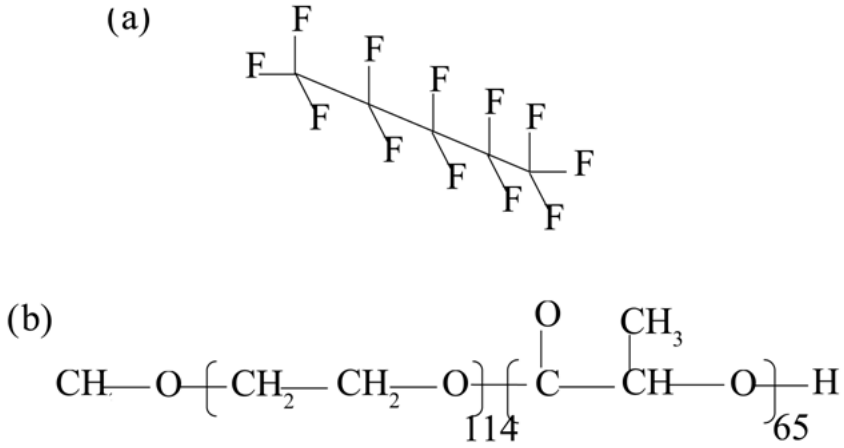

Figure 1: a) Structure of PFP. b) PEG-PLLA block co-polymer with 114 PEG units and 64 PLLA monomer units.

The micellar morphology was visualized using transmission electron microscopy (TEM). Figure 2b shows the TEM image obtained for 0.25% PEG-PLLA polymer solution. Two groups of micelles were observed. The size of smaller circular structures (Figure 3b) matched the size distribution of smaller micelles observed in the solution of the same concentration characterized by dynamic light scattering (peak of 18.1 + 3.2 nm in Figure 2a). Elongated lamellas in the TEM image likely correspond to the population of larger micelles seen in the size distribution obtained by dynamic light scattering (peak of 96 + 20.9 nm in Figure 2a).

PLLA forms a hydrophobic core with the hydrophilic PEG chains forming the outer shell. Surfactants reduce the surface tension of the PFP-water interface, which increases the coalescence time [7]. For non-ionic surfactants like PEG-PLLA, repulsive force is of entropic nature (steric repulsion) [8]. The polymer layer at the interface experiences a decrease in entropy when two droplets or bubbles approach each other. A decrease in entropy is not thermodynamically favorable, and therefore repulsion occurs [9]. Therefore these droplets stabilized by surfactants remain stable at room temperature.

The developed method for the preparation of the stabilized PFP emulsion starts with the formation of the polymer solution of the stabilizing agent. Solution of 2.5% (w/v) PEG-PLLA

(5000 Da molecular weight of the PEG block and 4700 Da of the PLLA block; purchased from Polymer Source, Quebec, Canada) was prepared by first dissolving the polymer in Tetrahydrafuran (THF). Filtered water was then added to the polymer in THF solution to get an aqueous solution of 0.5% (w/v) PEG-PLLA. This solution was transferred to a membrane tube (SpectraPor, Spectrum Laboratories Inc, Rancho Dominguez, CA) with a molecular cutoff of 3500Da. The organic solvent was removed by dialysis against water. The dialysis was repeated three times, with the final dialysis against phosphate buffered saline solution (PBS). PBS was added to the dialyzed solution to replace the lost volume and form the final 0.5% (w/v) PEG-PLLA solution. From here on, all copolymer concentrations are reported in w/v percentages. After preparation, the solution was refrigerated until use. The formulation was later diluted with PBS to obtain desired concentrations.

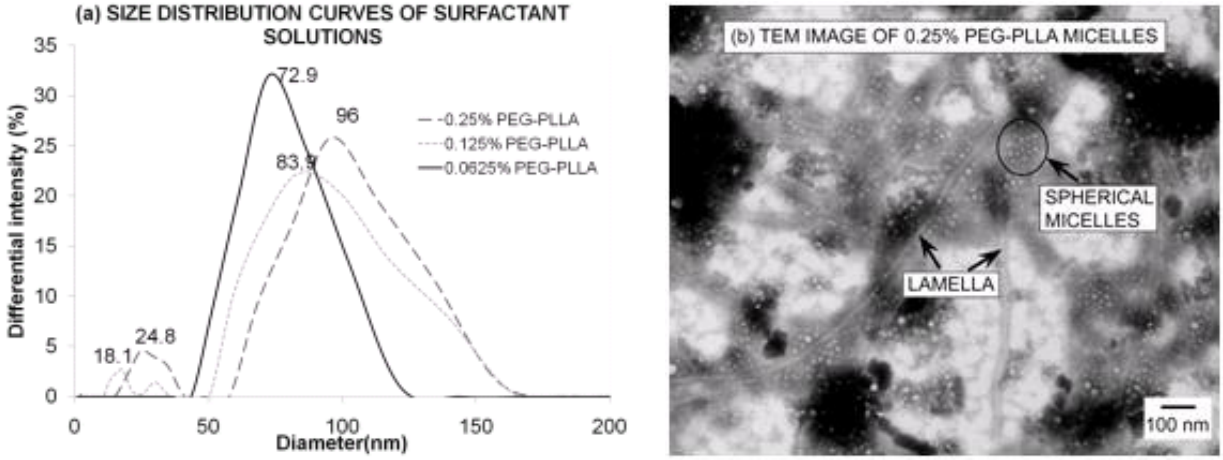

Figure 2: a) Normalized size distribution curves for 0.25%, 0.125% and 0.0625% PEG-PLLA micelle formulations measured using dynamic light scattering method at 25 ºC. Peak values are marked for each distribution. b) TEM image of the 0.25% PEG-PLLA solution showing micelles of size varying from 15 to 25 nm, and lamella structures.

To prepare the emulsion, using a pipette tip cooled to ~10 ºC, 5 ml of polymer solution was placed in a cooled container and liquid perfluoropentane (C_5F_{12}) (Fluoromed, Round Rock, TX) was added to obtain a 2 % (v/v) PFP–copolymer composition. The PFP-aqueous solution composition in this report is always reported as v/v percentages. The mixture was stored on ice to prevent PFP loss due to its high vapor pressure and low boiling point (~29 ºC). The emulsion was prepared by sonicating the mixture at 20 kHz using an immersed ultrasound probe (cup-horn installation, Sonics, Newtown, CT). The sonication was continued for approximately 1 min until the entire sample attained a milky appearance. The ultrasound exposure was carried out below room temperature by placing the sonication chamber on ice.

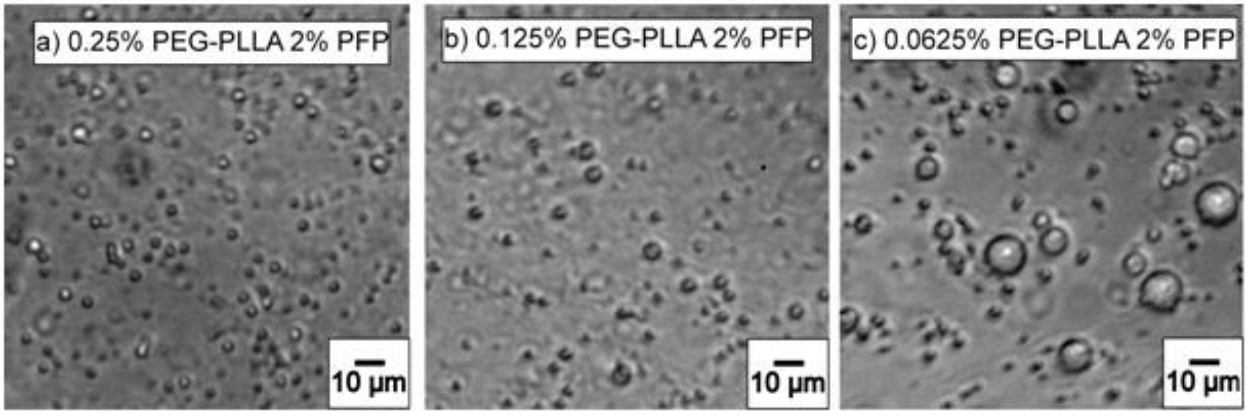

Figure 3: PFP emulsions with different surfactant concentrations

Task 2: Investigate factors affecting the size of PFP droplets in the emulsion

Different sonication frequencies and powers (ranging from low-power 20kHz cell disruptor to 660kHz high-power sonication inside sonochemistry apparatus (UES 5-660 Pulsar, Ultrasound Energy Systems, Fl) were used and the effect on the size distribution of the PFP nanodroplets in the emulsion were examined. It was found that higher sonication frequency and ultrasound power favor formation of smaller droplets until a limit controlled by the concentration of the stabilizing agent was reached. Figure 3 shows representative microscopy images of the emulsion obtained with different surfactant concentrations.

Size distribution of PEG-PLLA micelles and PFP emulsions were analyzed using dynamic light scattering (Delsa Nano S, Beckman Coulter, BREA, CA), which produced reliable size measurements in the range from 0.6 nm to 7 µm. Scattered light intensity measurements were analyzed using an autocorrelation method and the size distribution curves were obtained by fitting the measured autocorrelation functions using non-linear least squares method. Droplets larger than 1 µm precipitate from the suspension and thus cannot be reliably measured using light scattering. Thus the size of larger droplets was characterized microscopically, using a hemocytometer.

Morphology of PEG-PLLA micelles formed in the solution was characterized by transmission electron microscopy (Tecnai 12, FEI, Hillsboro, OR). A small volume (10 µL) of the surfactant solution of concentration 0.25% PEG-PLLA was placed on a 200 mesh carbon grid coated with Formvar carbon film (200C-FC, Electron Microscopy Sciences, Hatfield, PA). The solution was allowed to dry for 15 minutes, and the excess solution was absorbed with a filter paper. 10 µL of phosphotungstic acid was added on the grid to stain the micellar structures. Staining time was for 30 seconds after which the excess solution was removed using a filter paper. The grid was then placed in the vacuum chamber of the TEM, subjected to an accelerating voltage of 120 kV, and imaged. Morphology of droplet residues from 0.25% PEG-PLLA 2% PFP emulsion solution was also visualized using TEM by employing previously described method.

Table 1: Properties of perfluoropentane

Property	**Perfluoropentane**	**Perfluoro-15-crown-5-ether**
Average Molecular Weight:	288 g/g-mole	580.01 g/g-mole
Boiling point, T_b	29 °C	145 °C
Liquid Density, 25 °C:	1.63 g/mL	1.78 g/mL
Liquid Density, 35 °C:	1.59 g/mL	
Vapor Density, 1 atm:	10 (air = 1)	

Figure 4 shows the size distribution of the observed droplets, where the 400 nm diameter cutoff reflects the resolution limit of optical microscopy. The average sizes calculated from the distribution was 1.2 µm for 0.25% PEG-PLLA stabilized droplets, 1.22 µm for 0.125% PEG-PLLA stabilized droplets and 1.29 µm for 0.0625% PEG-PLLA stabilized droplets. Higher surfactant concentration favored partitioning of the PFP phase into numerous small droplets of 1 µm diameter and smaller (Figure 4a and b). Higher number of droplets of size larger than 5 µm was observed in 0.0625% PEG-PLLA emulsion (Figure 4c).

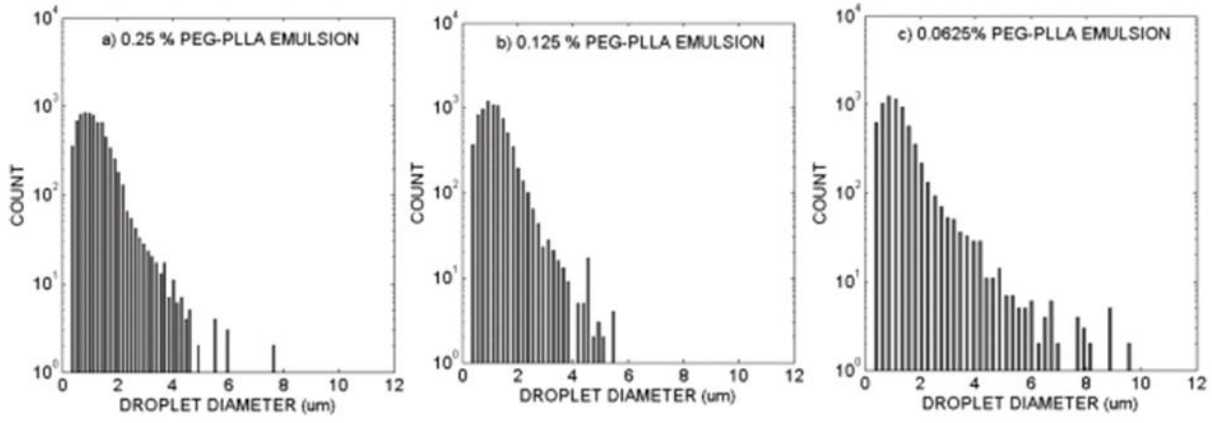

Figure 4: Droplet size distribution in 2% PFP emulsions with different PEG-PLLA concentrations.

Dynamic light scattering was used to characterize droplet sizes below the resolution of optical microscopy. The droplet size distribution measured by DLS (Figure 5a) shows the presence of two droplet size populations. After drying the emulsion sample of 0.25% PEG-PLLA 2% PFP on the carbon grid, the TEM image (Figure 5b) shows coronal residue of the PEG-PLLA surfactant

preserved on the surface after droplet evaporation. The image confirms the presence of droplets of the two populations of droplet sizes consistent with DLS measurements.

Prior to acquiring DLS measurements, the sample was allowed to equilibrate for 2 minutes during which rapid precipitation of larger droplets, seen in Figure 3, was noted. The range of sizes affected by precipitation was estimated using Stokes law, which gives the terminal velocity of droplets sedimentation as $v = \frac{gd^2}{18\mu}(\rho_S - \rho)$, where d is the droplet diameter, μ is the shear viscosity of the surfactant solution, ρ and ρ_s are the PFP and solution densities, respectively. Using the manufacturer reported PFP density (Table 1) and the measured value of μ (as described below), it was found that during 2 minutes of equilibration 10 µm droplets, precipitating at the terminal velocity, travel approximately 4 mm. Due to this precipitation, the distribution of large PFP droplets (above 2 µm) measured by dynamic light scattering was not accurately obtained, while the effect of precipitation on the size measurements for droplets less than 1 µm was negligible. Consequently, the measured size distribution of larger droplets, affected by sedimentation, is better characterized by optical techniques (Figure 4) for particle sizes larger than 2 µm. Both techniques indicate that higher surfactant concentration favors formation of smaller droplets.

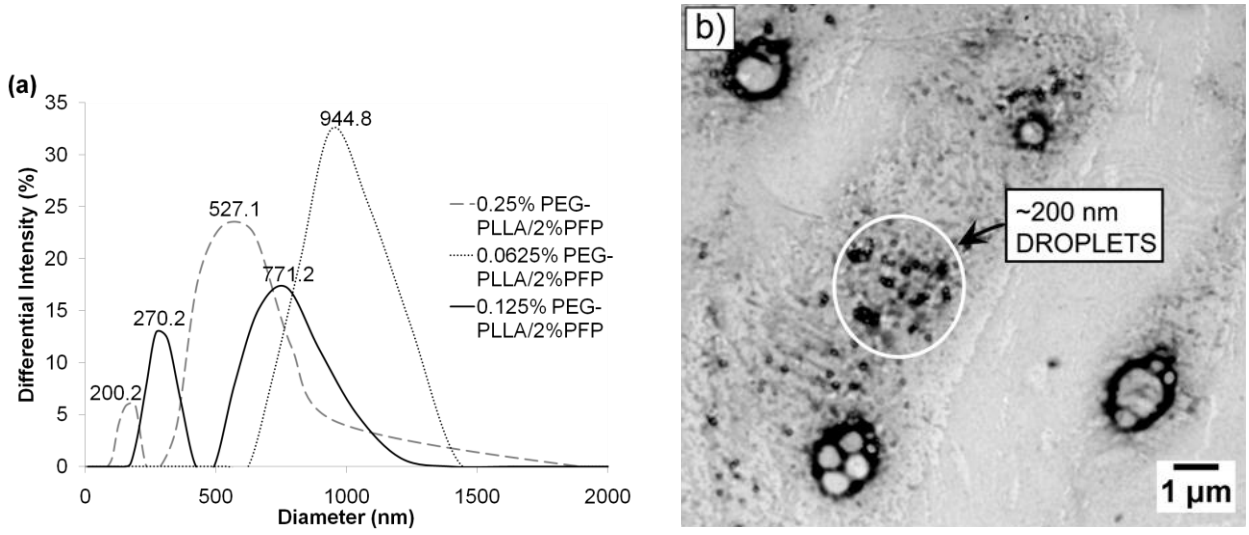

Figure 5: a) Normalized droplet size distribution curves with the corresponding peak diameter values obtained by dynamic light scattering at 25 ºC. b) TEM image of droplet residue shows two different size distributions of approximately 200 nm and 1 µm.

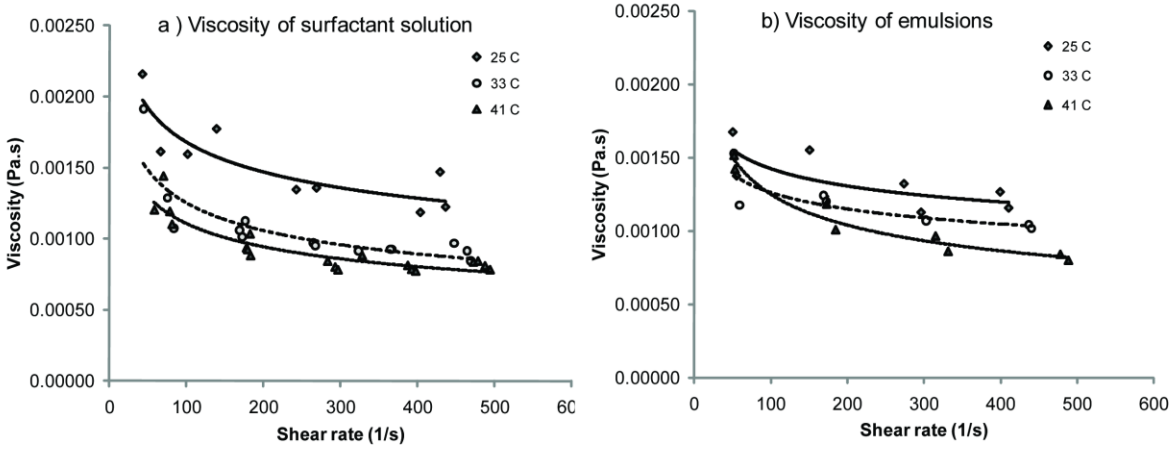

Figure 6: a) Viscosity of surfactant solution (0.25 % PEG-PLLA) as a function of shear rate. Shear thinning behavior is observed and viscosity decreases as temperature increase from 25 to 33 and 41 °C. b) Emulsion (0.25% PEG-PLLA 2% PFP) viscosity as a function of temperature.

Shear viscosity of emulsions and surfactant solutions were individually measured using a cone and plate rheometer (AR550 constant stress rheometer, TA Instruments, New Castle, DE). The sample was placed on the horizontal plate and a ~1 degree shallow cone was rotated to shear the sample with a known shear rate. A shear sweep experiment was conducted by varying the shear rate from 0 to 500s-1 by controlling the rotational speed of the cone. The torsional force needed to maintain the rotation was measured and used to estimate the corresponding shear stress in the sample. Temperature of the rheometer plate was controlled to obtain viscosity curves at different temperatures ranging from 25 to 45 °C.

Figure 6 shows the measured viscosities as a function of shear rate and temperatures. Viscosity of the surfactant solution (0.25 % PEG-PLLA) decreased with an increase in shear rate, indicating shear thinning behavior (Figure 6a). While measuring emulsion viscosities (0.25% PEG-PLLA 2% PFP), the PFP evaporated quickly thereby reducing the sample volume, and decreasing the number of droplets. Due to PFP evaporation, with time the viscosity of the emulsion will approach the values obtained for surfactant solution. Figure 6b shows the measured viscosity of the emulsion for the case when low shear rate measurements were obtained first and then proceeding to the higher shear rate values. The result indicates that the presence of PFP droplets tends to decrease the viscosity. It also shows that with time, as PFP evaporates the measured viscosity values at higher shear rates approach those observed with the surfactant solution. The measurements were repeated for different temperatures 25 °C, 33 °C and 41 °C. Viscosity curves shifted down at higher temperatures indicating decrease in viscosity with temperature increase.

Surface tension is the key factor affecting the dynamic response of emulsion to external triggers. Interfacial tension of PFP was measured using pendant drop method [10].The experimental setup is depicted in Figure 7. The system contains a 5 ml glass syringe with an interchangeable needle with steel luer-type connector and a ground glass stopper (Hamilton Company, Reno, NV). The

needle tip was placed inside a temperature controlled test chamber. A drop of PFP was formed by injecting PFP through the needle into the chamber. The shape of the PFP drop was imaged using a 10 X microscope magnification (Melles Griot, Irvine, CA) and captured with a CCD camera (MS-4030, Sierra Scientific, Los Angeles, CA). The CCD camera was connected to the computer using a digitizing card. The first image was captured 5-10 s after the formation of the drop. The radii of curvature of PFP drops were determined from the image using Image 1.37 software. The PFP surface tension and its interfacial tension against aqueous solutions were obtained by finding the best match between the imaged droplet shape and the theoretical prediction of its shape obtained by solving the differential Laplace-Young equation with an estimated PFP tension, detailed in reference [11] and the Appendix.

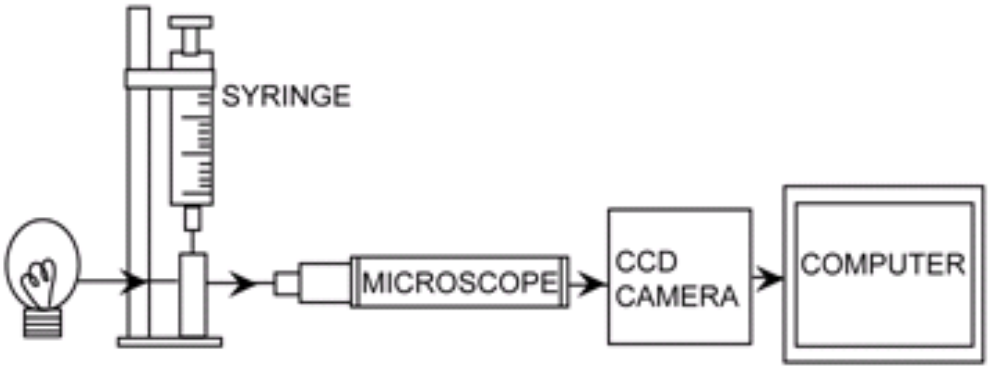

Figure 7: Setup of pendant drop method

To validate our experimental procedure for the pendent drop method, interfacial energies of PFP-air, PFP-water and PFP-PBS were measured and compared with the reported values, which are 55 dynes/cm for PFP-water interfacial tension and 9.5 dynes/cm for surface tension. It was found that our measurements closely match literature values. The pendant drop method was then used to measure the interfacial tension of PFP against the surfactant solution (0.25% PEG-PLLA) at different temperatures. Figure 8 shows the average values of measured surface tension and interfacial tension values of PFP. The results of Figure 8 show that interfacial tension of PFP-PEG-PLLA solution was significantly lower than interfacial tension values of PFP-PBS system, indicating a stabilizing effect of block copolymer surfactant. Interfacial tension of PFP against varying concentrations of PEG-PLLA and other surfactant solutions has been reported in [11].

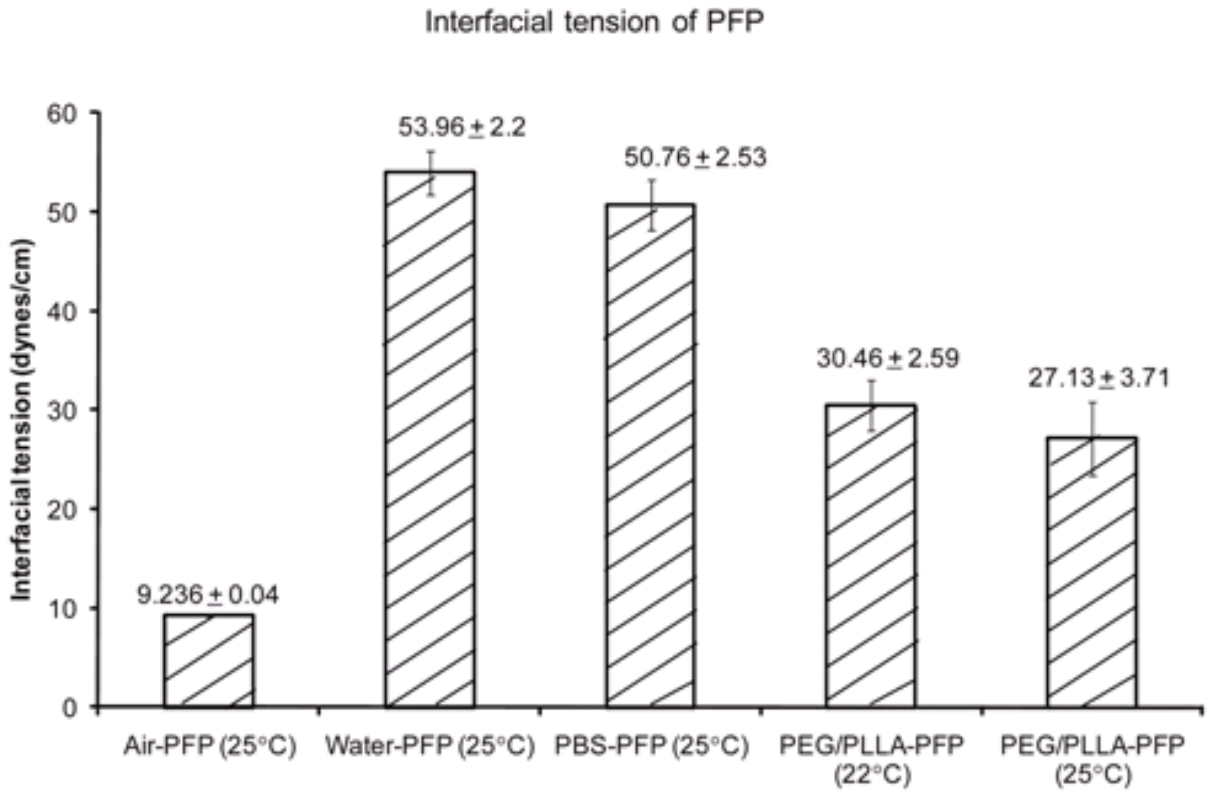

Figure 8: Surface and interfacial tension of PFP against water, PBS and 0.25% PEG-PLLA surfactant solution at 22 and 25 °C.

Task 3: Characterize oxygen release from stabilized PFP droplets

We investigated several compounds as fluorescent oxygen probes intended to characterize the release of oxygen from the PFP emulsion carriers. We found that fluorescence of Ruthenium compounds (such as tris-(2,2'-bipyridine) ruthenium (II) dichloride) are readily quenched by dissolved oxygen and are therefore suitable for characterization of the oxygen release from the carriers. As an illustration, Figure 9a shows the fluorescent image of the degased solution of the oxygen probe. As long as dissolution of the oxygen is avoided, the steady fluorescent intensity was maintained. However, when the PFP emulsion, prepared and equilibrated to allow for the oxygen saturation, was added to the solution, the fluorescent intensity decreased in the immediate proximity of the oxygen-saturated PFP droplets (Figure 9b) indicating the release of the oxygen into the solution. The decreased intensity spread with time, indicating oxygen transport by diffusion and confirming our conclusion that the selected class of compounds can be used to characterize the release of O2 from the carriers.

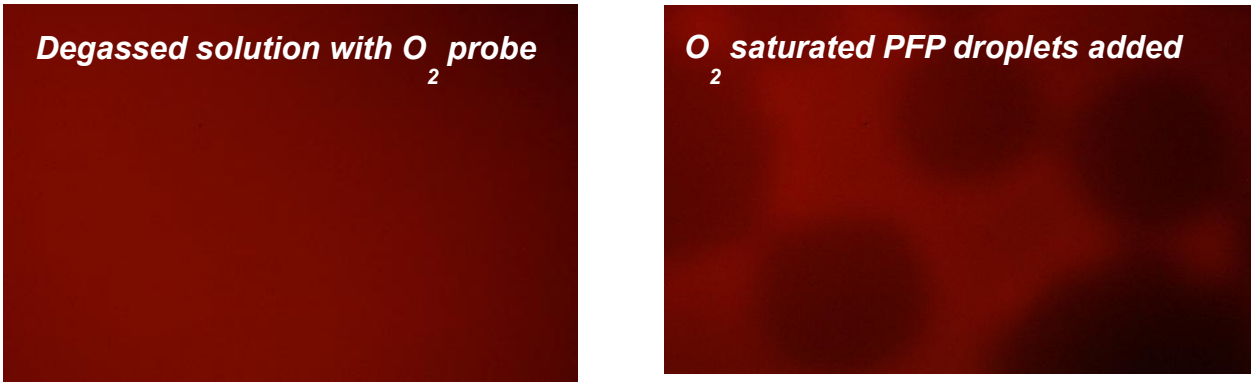

Figure 9: Effect of oxygen release on the fluorescent intensity.

Task 4: The effect of elevated temperature, reduced pressure and radiation on phase transition of carriers

We investigated the effect of different stimuli on the dynamics of the PFP emulsion, including phase transition. Optical microscopy (Nikon Fluophot, Nikon Microscope Inc, Melville, NY) was used to characterize the response of the stabilized PFP emulsion to elevated temperatures. The emulsion samples were injected into microfluidic 640x640 μm square channels made of cyclo-olefin copolymer (COC) (ThinXXS, Germany), and placed on the microscope stage. The temperature was changed in step increments from ambient to 50ºC using an external heated air flow, set at different flow rates. The surface temperatures of the top and bottom surfaces of the microfluidic chip were measured using needle thermocouples (Type T, Physitemp, Clifton, NJ). The channel temperature was estimated as an average of the two surface temperatures. After each change in the flow of heated air, 5 minutes were allowed for the measured temperature of both channel surfaces to stabilize. The data were collected at temperatures ranging from 25 ºC to 50 ºC. The transitional behavior of microdroplets and formed microbubbles was captured using a digital camera (Nikon D200, Nikon Inc, Melville, NY) mounted on the microscope. Both concentration and temperature dependence of the size of the microbubbles were visualized. Experiments were repeated for various PEG-PLLA concentrations.

The formation of microbubbles in 0.25% PEG-PLLA/ 2% PFP emulsion was also thermally imaged in the same 640x640 μm square microchannel maintained at 50 °C by a heating stage. An evolving temperature distribution in the emulsion with the spatial resolution of 5 μm spot size was captured using a highly sensitive (sensitivity of better than 0.025°C) infrared microscopy camera (Silver SC5000, FLIR Systems, Willsonville, OR).

In experiments, the surfactant solution with no PFP phase present was used as a control. After initial injection into 640 x 640 μm microfluidic channel microscopic observation indicated that no bubbles were present and, after increasing the channel temperature to 45 ºC, no new bubbles were formed.

Temperature response of PFP emulsions with 0.25% PEG-PLLA solution was imaged, with the results obtained shown in Figure 10. After injecting the emulsion into the channel at the room temperature, a few small bubbles were seen inside. The reduced surface tension and the reduced

dynamic pressure created during the injection of the emulsion into the channel are the likely causes of the initial bubbles formation prior to heating. During heating experiments, the microchannel temperature was allowed to equilibrate, and different sections throughout the channel were then imaged, with two sections shown in Figure 10. The temperature settings were changed sequentially from low to high. Once the target temperature was reached, the channel was equilibrated for five minutes, and then imaged, which took another five minutes to complete.

The experiment was repeated for the emulsions formed with the following concentrations of PEG-PLLA: 0.25%, 0.125%, and 0.0625%. The number of microbubbles formed at each temperature increment and the average microbubble volumes were calculated from all images of different sections of the channel, averaged and plotted as a function of temperature in Figures 11 and 12, where the error bars are equal to 95% confidence interval values. Increase in temperature leads to an increase in the volume of the microbubbles observed prior to heating, and the formation and growth of new microbubbles, as shown in Figure 10. The observed growth of the number of microbubbles, which captures the competing effect of new bubble formation and bubble coalescence, is approximately linear for the temperatures in the investigated range. The average radius of the microbubble grows with temperature and time. Therefore, the results of Figures 11 and 12 give the cumulative effect of these two factors.

The temperature response was similar for PEG-PLLA concentrations of 0.25% and 0.125%, with the exceptions that the new number of bubbles formed was slightly higher for 0.125%, and the increase in average bubble radius with temperature was slightly lower for 0.125%. There was a significant increase in the average bubble radius when the concentration of PEG-PLLA was 0.0625%. The total number of bubbles decreased with 0.0625% PEG-PLLA concentration, where small number of very large bubbles was observed.

To observe the contribution of PFP and dissolved gases in the solution to bubble formation and growth, total volume of bubbles in the channel were calculated for all concentrations of PEG-PLLA at different temperatures, shown in Table 2. Table 2 shows increase in total volume of bubbles with temperatures, as well as the significant increase in the volume when the concentration of PEG-PLLA was 0.0625%.

The effect of time on the growth of the bubbles in a microchannel was examined separately with the 0.25% PEG-PLLA stabilized emulsions and the results are summarized in Table 3. At 26 °C, the initial bubbles population present prior to heating grew over time, with the 10 min increase shown in Table 3. A rapid temperature increase from 26 °C to 45 °C resulted in a 1000 fold increase in an average microbubble volume. After 10 minutes of holding temperature at 45 °C, the average volumes of microbubbles further increased by a factor of 1.8, which is substantially higher than the average volume increase at 26 °C over the same time. The initial number of bubbles in the channel formed after injection of the sample is dependent on the injection, and the pressure created inside the channel. It varies between different experiments, and also affects the new bubbles formed at higher temperatures.

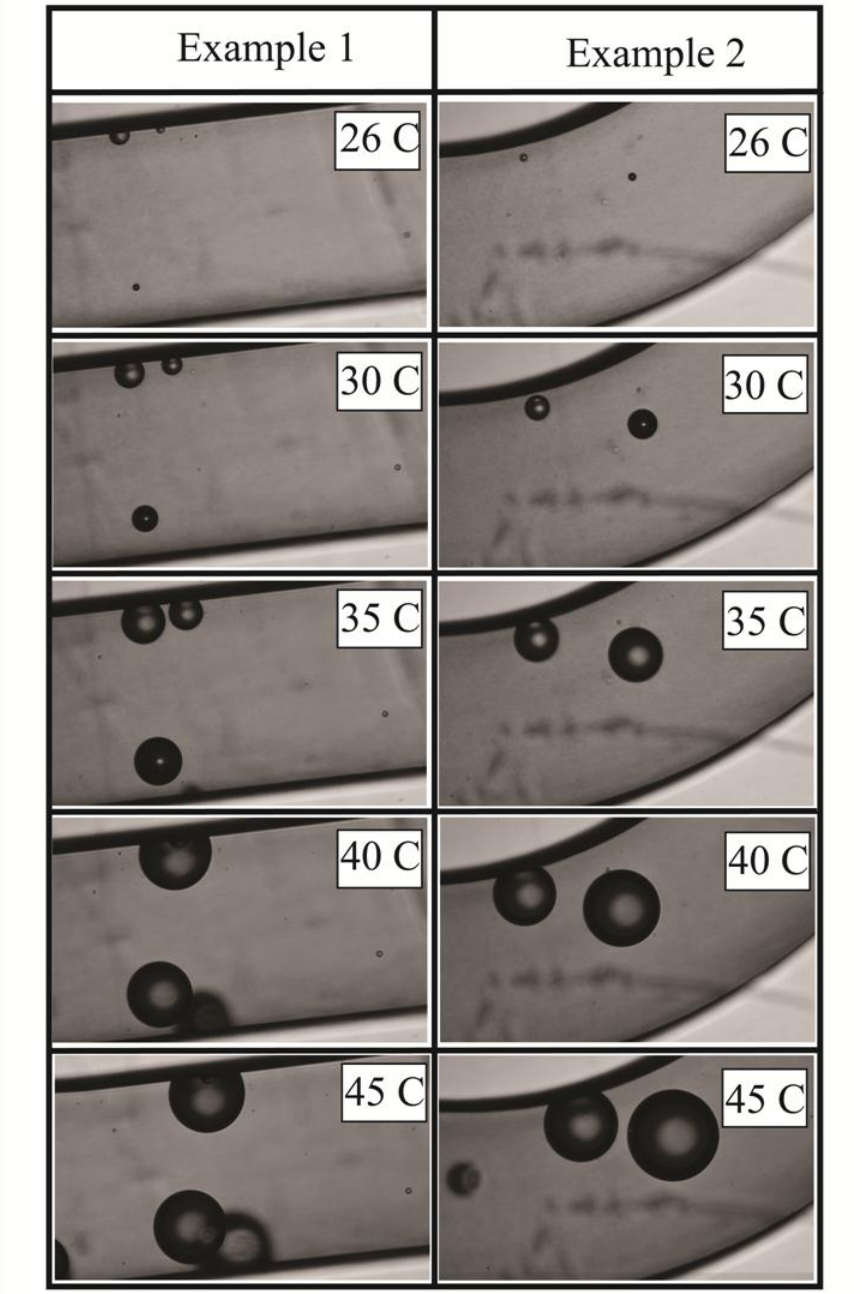

Figure 10: Effect of temperature on the microbubble formation and growth in a 640x640 µm square channel containing 0.25% PEG-PLLA stabilized PFP emulsion.

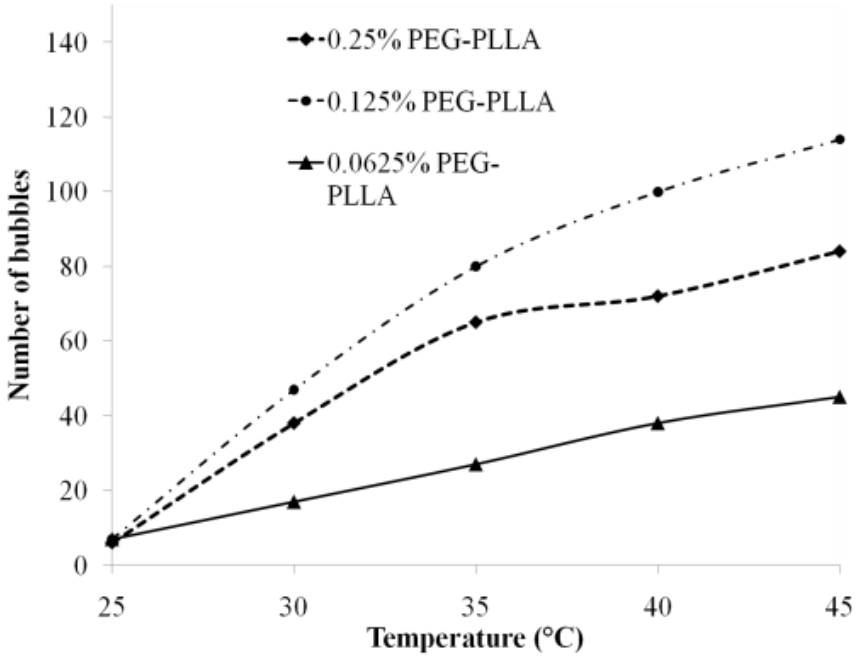

Figure 11: Increase in the number of microbubbles plotted against temperature for PFP emulsions stabilized with PEG-PLLA at different concentrations.

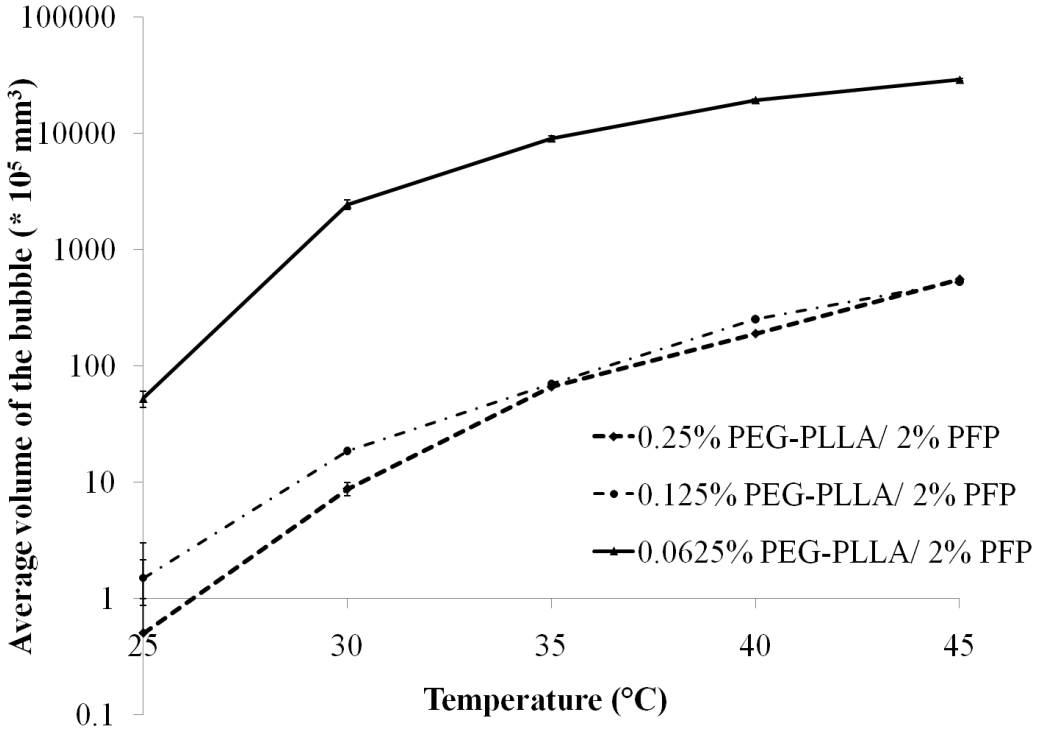

Figure 12: Increase in average volume of bubbles as a function of temperature.

Table 2: Total volume of the bubbles calculated for different concentrations of PEG-PLLA at different temperatures of the microchannel

Temperature (°C)	Total volume of the bubbles calculated as the number of bubbles times average volume of the bubbles ($*10^{-5}$ mm^3)		
	0.25% PEG-PLLA/ 2% PFP	0.125% PEG-PLLA/ 2% PFP	0.0625% PEG-PLLA/ 2% PFP
25	0.50	1.5	52.21
30	0.88	18.6	2434.62
35	66.13	70.25	9016.05
40	189.36	251.9	19258.64
45	555.64	529.6	28783.73

Table 3: Increase in volume of the bubbles for (0.25% PEG PLLA/2% PFP) emulsion was tracked over a time of 10 minutes at 25 and 45 °C, and the average volumes were calculated, with $\pm$ 95% CI. The numbers of bubbles used for calculating the averages are tabulated as n in the Table.

Temperature (°C)	Average volume (mm^3) at t = 0 min	Average volume (mm^3) at t = 10 min
25	$4.05 *10^{-5} \pm 2.6 *10^{-5}$ n = 15	$1.06 *10^{-4} \pm 3.98 *10^{-5}$ n = 18
45	0.01 ± 0.0037 n = 11	0.018 ± 0.0047 n = 11

To characterize the response of the PFP droplets to the change in pressure, Emulsion was injected into a 640 micrometer square microfluidic channel. The channel was then sealed with the exception of one port which was connected to a pressure regulator (PV830, Pneumatic PicoPump, WPI). With the pressure regulator connected to house vacuum, the pressure within the channel could be adjusted from 0 to -15 inHg.

The channel was observed using light microscopy at 400 X magnification. For each pressure experiment, digital photographs of the initial state of the emulsion at STP were taken along the microfluidic channel. The pressure within the channel was then reduced to -5, -10, or -15 inHg, and images were collected approximately every 5 minutes. At the end of 30 minutes, the pressure within the channel was returned to atmospheric pressure, and a final set of images were taken.

Bubble dimensions were determined using standard image analysis functions found in Matlab's Image Processing Toolbox. To distinguish bubbles from those with which they were in contact, a watershed algorithm was used.

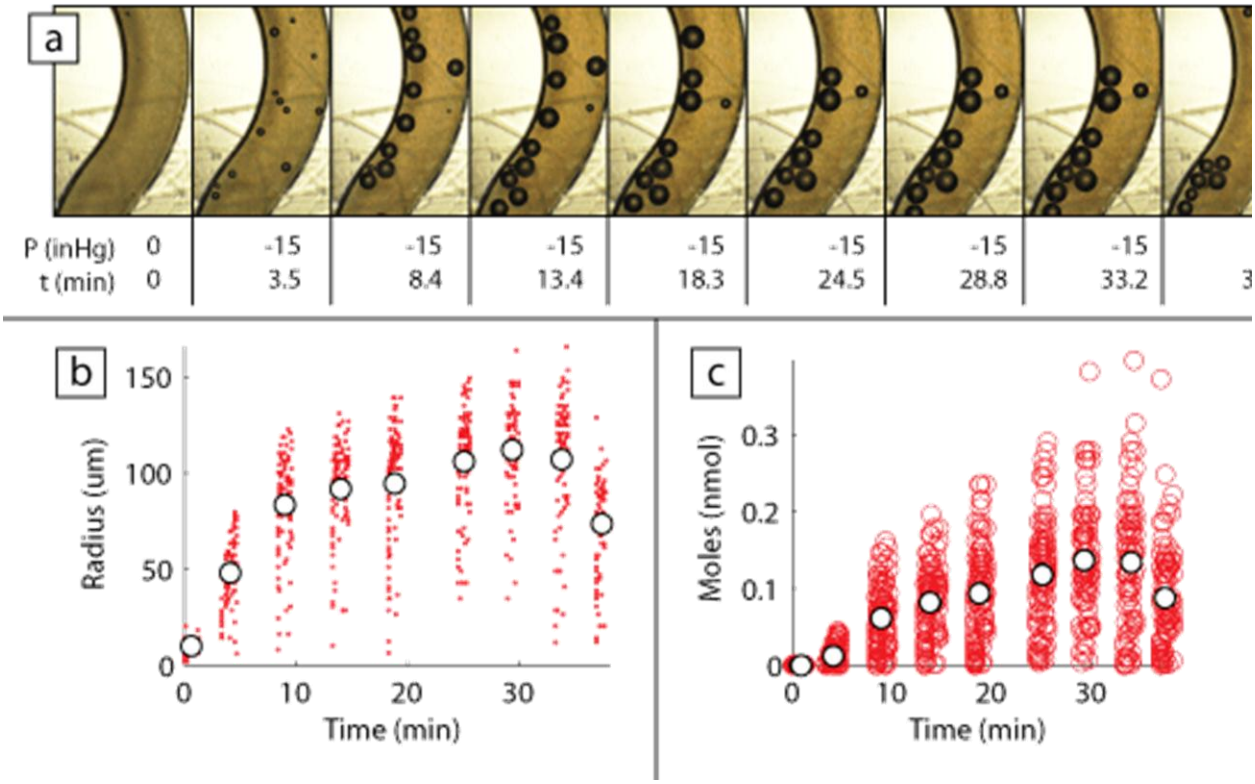

Figure 13: Data from a typical experimental run. a) Sequence of images to be analyzed. b) Bubble radius (dots) and average radius (circles). c) Moles of gas within bubbles (red circles) and average moles (filled white circles).

Figure 13 illustrates a typical experimental run. Figure 13a shows a sequence of images of our emulsion in the microchannel taken approximately every 5 minutes. Throughout the experimental run, 11 separate segments of the microchannel were imaged in a similar manner. At time equals zero the pressure in the channel was dropped from atmospheric to -15 inHg in this instance, and the bubble dimensions were tracked (Figure 13b and 13c). At approximately 30 minutes, pressure was returned to atmospheric and the final set of bubble measurements was taken. As was common to all experimental runs and may be seen in Figure 13a, b and c, when returned to atmospheric pressure bubbles merely diminished in size and the system did not return to a bubble-free state, indicating the bubbles are a mixture of PFP and dissolved gases. However, bubbles were seen to shrink more than what would be accounted for using a gas law, indicating gasses did dissolve into the aqueous phase, in part.

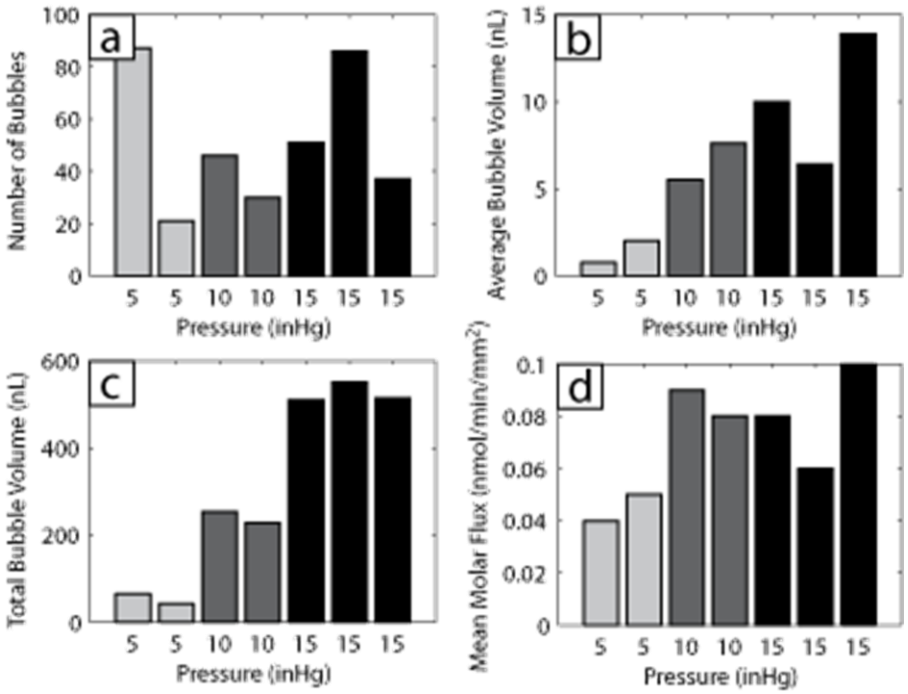

Figure 14: a) Number of bubbles observed. b) Average bubble volume. c) Total bubble volume. d) Average molar flux in to the gas phase per bubble surface area.

Experimental results at three reduced pressures, -5 inHg, -10 inHg, and -15 inHg are shown in Figure 14. Figure 14a shows the number of bubbles created. It appears the extent to which pressure is decreased is largely unrelated to the number of bubbles produced, suggesting bubble growth depends more upon the presence of nucleation sites. Furthermore, histograms of bubble appearance locations were found to better match the probability density function predicted by nucleation occurring solely on the channel walls, verses within the bulk emulsion, again suggesting a necessity of nucleation sites for bubble growth at all pressures examined. It is also important to note that the vast majority of bubbles are formed at the time the pressure is decreased, with less than 10% of observed bubbles appearing after such time.

From Figure 14b it is apparent that bubble size after 30 minutes at room temperature and depressed pressure depends upon both the pressure and the number of bubbles present (or the number of initial nucleation sites). However, as seen in Figure 14c, the total gas volume in the system is proportional to the pressure drop and is only slightly correlated with the initial number of bubbles. Figure 14d shows the average molar flux from the liquid into the bubbles, taking Laplace pressure into consideration and assuming the ideal gas law holds. As the number of bubbles increases, the molar flux decreases, suggesting bubble growth is determined by dissolved gas concentration. It seems, from Figure 14, that the pressure and the number of nucleation sites ultimately determine the average bubble volume and rate of growth.

A control experiment without PFP found no bubble growth, even at -15 inHg and 50 C. However, an experiment with the PFP emulsion which was allowed to run over 5 days at room temperature and atmospheric pressure found slow bubble growth with an average molar flux of

0.001 nmol/min/mm2, less than an order of magnitude below the values seen at -5 inHg. That experiment at atmospheric pressure was necessarily terminated as the channel filled with bubbles, crowding out the emulsion and making bubble volume estimations difficult after 4 days. Alternatively, when emulsions are closed off to the air, they eventually halt bubble growth.

At room temperature pure PFP was found to boil at -7 inHg, though only when nucleation sites were present. At -23 inHg, the lowest pressure that we could achieve, PFP would not boil without a nucleation seed. As the droplets in the emulsion are near perfect PFP spheres surrounded by a surfactant shell, it is highly unlikely nucleation could occur within them. The observed bubble growth is therefore not likely to be due to the transition of single droplets into vapor by boiling at our experimental conditions. However, the solubility of PFP in water is very low, thereby ruling out diffusion of PFP from droplets through the aqueous phase and into bubbles as the predominant means of bubble growths.

The effect of radiation on the bubble formation was studied with cesium source of different intensities. The addition of the radiation, separately and in combination with the elevated temperature and/or reduced pressure, had no statistically significant effect on the observed dynamics of the stabilized PFP emulsions.

Task 5: Effect of radiation localization

In our approach, we proposed to oxygenate cancerous tissues prior to X-ray treatment to improve the efficacy of the radiation therapy. While the triggering of the oxygen release from PFC carriers is effectuated by elevated temperature and/or reduced pressure, our objective was also to conduct a preliminary investigation on the effect of the radiation on the dynamics and, specifically, phase transition, of the oxygen carriers. While it was never expected that radiation can provide sufficient energy to cause phase transition of PFP droplets, we allowed for the possibility that radiation may enhance the process by creating nucleation sites that are the necessary condition for the phase transition. Our experiments indicate that radiation has no effect on phase transition when the emulsion is below the boiling point temperature and pressure of the PFP droplets (accounting for the elevated pressure inside the droplets dues to surface tension effects – the Laplace pressure), indicating that, indeed, radiation alone does not trigger the phase transition. When we investigated the phase transition at elevated temperatures and pressures, surprisingly the addition of the radiation also had no statistically significant effect. This observation can be explained by the presence of sufficiently large number of nucleation sites in the solution (such as micelles formed PEG-PLLA stabilizer, microscopic dust particles and very small gas bubbles) and the surface of microfluidic channels (due to the roughness of the surface and trapped microscopic gas bubbles) in which the experiments were conducted. Under these circumstances, the suspension cannot be brought up to supercritical condition (because phase transition occurs prior to this happening) at which radiation can be expected to contribute to the formation of additional nucleation sites. It appears reasonable to assume that sufficient number of nucleation sites will be present in vivo and radiation will have no or limited effect on the phase transition of oxygen carriers in patients.

Task 6: Oxygen release during and after phase transition

After characterizing the phase transition in response to the elevated temperature, reduced pressure, radiation and the combination of these factors, the dynamics of the oxygen release

during and after the phase transition was observed microscopically. Surprisingly, reduced pressure and elevated temperature never resulted in the direct observation of the transition of a given PFP droplet to a bubble despite a very large number of experiments carried out to observe such transition. For example, at -23 inHg of negative pressure, which is the lowest pressure that we could achieve with our setup, PFP droplets that we were observing would not boil and undergo phase transition, both of which are the processes that require nucleation sites for their initiation. As the droplets in the emulsion are near perfect PFP spheres surrounded by a surfactant shell, it is highly unlikely nucleation site could occur within them, which would explain why we were not able to observe the phase transition of any given PFP droplet. Instead, the bubble formation, we hypothesize, always starts at an unknown nucleation site, which is likely a microscopic air bubble, a micelle, dust particle, or imperfection on the channel wall -- all below the resolution of our optical microscope (1000x limit). The formed bubbles start very small and rise into in the focal plane of the microscope, where they are observed for some time (typically few seconds) before rising out of focus. Because the location of the formed and growing bubbles was unpredictable and bubbles rose during the experiment, the direct observation of the effect of the phase transition on the release of the oxygen from the carriers was not possible in our experimental setup. However, the background florescence was quenched substantially faster during the process of the bubble formation and growth compared to the quenching observed due to oxygen transport to the solution from droplets at room conditions (Fig. 9). This result provides indirect support to our hypothesis that phase transition enhances the release of the oxygen from the carriers triggered by heating and sonication.

Key research accomplishments

1. The method to produce sterically stabilized perfluorocarbon oxygen carriers has been developed. This method can produces droplets 5 um in diameter or smaller, a clinically relevant range. These droplets can be loaded with dissolved oxygen at very high concentration, up to 80 vol% and remain stable during prolonged storage when kept in refrigerator.
2. The dynamic response of the oxygen carriers in response to an elevated temperature, reduced pressure, and radiation has been characterized and factors that influence the response were determined. It was found that both temperature and pressure have a significant effect on the carriers, their size and phase transition.
3. We have established that ruthenium compounds can be used as florescent oxygen probes to characterize the oxygen release from the carriers.
4. It was found that oxygen slowly diffuses from the PFP droplets into the solution. Based on our initial results, we believe that the rate of such release can be controlled by the surfactant selection and by changing the concentration of the surfactant on the surface of the droplets.
5. Preliminary results provide initial evidence that carrier phase transition, externally triggered by an elevated temperature in a physiologically mild range (41-50C) and reduced pressure, accelerates the release of the oxygen from the carriers. Both of these external excitations can be targeted and applied non-invasively using focused ultrasound, which creates a potential to trigger oxygen release non-invasively, prior to the radiation therapy.

Reportable outcome

- One paper partially based on the results of this research has been already published [11 and Appendix] and two more (describing the temperature and pressure responses of the PFP emulsions) are currently in preparation.
- Three presentations were made [12-14] to disseminate the results.
- A patent disclosure was filed with the University of Utah Technology and Commercialization Office.

Conclusion

This project was directed at the initial development of a novel strategy of radio sensitization of hypoxic breast tumors by targeted oxygen release from perfluorocarbon oxygen carriers. In the proposed approach, an emulsion of oxygen-saturated perfluorocarbon droplets, less than 5μm in diameter and as small as 100nm, was stabilized by a biocompatible amphiphilic block co-polymer PEG-PLLA. The proposed strategy is based on the hypothesis that the preferential release of oxygen from PFC droplets inside or in the proximity of the tumor can be achieved by targeted, localized heating and sonication. The preliminary results obtained during this project support our hypothesis and provide sufficient evidence to warrant further research and the development of the proposed approach.

References

1. Vaupel P, Briest S, Höckel M. Hypoxia in Breast Cancer: Pathogenesis, Characterization and Biological/Therapeutic Implications. Wiener Medizinische Wochenschrift 2002;152(13-14):334-342.
2. Gray LH, Conger AD, Ebert M, Hornsey S, Scott OC. The concentration of oxygen dissolved in tissues at the time of irradiation as a factor in radiotherapy. The initiation and development of cellular damage by ionizing radiations. British Journal of Radiology 1953;(26):638–648.
3. Clarke H, Pallister CJ, The impact of anemia on outcome in cancer. Clinical & Laboratory Hematology 2005;27(1):1-13.
4. Squires JE. Artificial Blood. Science, 2002;295(5557):1002-1005.
5. Shorr RG, Viau AT & Abuchowski A. Phase 1B safety evaluation of PEG hemoglobin as an adjuvant to radiation therapy in human cancer patients. Artificial Cells, Blood Substitutes and Immobilization Biotechnology 1996; 24(abstracts issue):407.
6. Pierri, E. and K. Avgoustakis, Poly(lactide)-poly(ethylene glycol) micelles as a carrier for griseofulvin. J Biomed Mater Res A, 2005. **75**(3): p. 639-47.
7. Slattery, J.C., Interfacial Transport Phenomena. 1990, New York: Springer.
8. Giribabu, K.a.G.P., Adsorption of nonionic surfactants at fluid–fluid interfaces: Importance in the coalescence of bubbles and drops Chemical Engineering Science, 2007. **62**(11): p. 3057-3067.
9. Ghosh, P.a.J., V.A., Analysis of the drop rest phenomenon. Chemical Engineering Research and Design, 2002. **80**: p. 715-728.

10. Tripp, C.B., Dynamic surface tensions of model protein solutions measured via pendant drop tensiometry, in Department of Chemicals and Fuels Engineering. 1993, University of Utah: Salt Lake City. p. 86-101.
11. Kandadai M., L.G., Mohan P., Butterfield A., Skliar M., Magda J., Comparison of Surfactants Used to Prepare Aqueous Perfluoropentane Emulsions for Pharmaceutical Applications. Langmuir, 26: 4655–4660, 2010.
12. Butterfield A., Mohan P., and Skliar, M., Pressure Effects On Bubble Growth in An Emulsion of Surfactant-Stabilized Perfluoropentane Micro-Droplets,' AIChE Annual Meeting, November 7-12, 2010, Salt Lake City, UT.
13. Mohan, P., Butterfield A., and Skliar, M., Temperature Response of Poly (L-lactide-co-ethylene glycol) Stabilized Perfluoropentane Micro-Droplets," AIChE Annual Meeting, November 7-12, 2010, Salt Lake City, UT.
14. Skliar, M., Investigation of Temperature and Pressure Response of Stabilized Perfluorocarbon Emulsions," Era of Hope, August 2-5, 2011, Orlando, FL.

Langmuir
Article
pubs.acs.org/Langmuir

Comparison of Surfactants Used to Prepare Aqueous Perfluoropentane Emulsions for Pharmaceutical Applications

Madhuvanthi A. Kandadai,*,† Praveena Mohan,‡ Genyao Lin,§ Anthony Butterfield,† Mikhail Skliar,† and Jules J. Magda†

†Department of Chemical Engineering, ‡Department of Bioengineering, and §Department of Materials Science and Engineering, University of Utah, Salt Lake City, Utah 84112

Received August 8, 2009

Perfluoropentane (PFP), a very hydrophobic, nontoxic, noncarcinogenic fluoroalkane, has generated much interest in biomedical applications, including occlusion therapy and controlled drug delivery. For most of these applications, the dispersion within aqueous media of a large quantity of PFP droplets of the proper size is critically important. Surprisingly, the interfacial tension of PFP against water in the presence of surfactants used to stabilize the emulsion has rarely, if ever, been measured. In this study, we report the interfacial tension of PFP in the presence of surfactants used in previous studies to produce emulsions for biomedical applications: polyethylene oxide-*co*-polylactic acid (PEO-PLA) and polyethylene oxide-*co*-poly-ε-caprolactone (PEO-PCL). Because both of these surfactants are uncharged diblock copolymers that rely on the mechanism of steric stabilization, we also investigate for comparison's sake the use of the small-molecule cationic surfactant cetyl trimethyl ammonium bromide (CTAB) and the much larger protein surfactant bovine serum albumin (BSA). The results presented here complement previous reports of the PFP droplet size distribution and will be useful for determining to what extent the interfacial tension value can be used to control the mean PFP droplet size.

Introduction

The unique physical, chemical, and biological properties of perfluoropentane (PFP, see Figure 1) have generated much interest for its use in several biomedical applications such as propellants for pressurized metered dose inhalers (pMDIs) for the direct delivery of drugs to the lungs,[1,2] for ultrasound contrast enhancement,[3] and for the transport of oxygen in vivo in artificial blood.[4−7] PFP also shows promise in the field of drug delivery and gene transfection.[8−11] Like almost all perfluorocarbons, PFP has a high capacity to absorb oxygen. More importantly, the normal boiling point of PFP lies between room temperature and body temperature. This means that PFP can be injected in the form of liquid droplets dispersed in an aqueous medium and then converted to bubbles using ultrasound. This conversion to bubbles can be used to release anticancer drugs such as doxorubicin at a site of interest[11] or to occlude blood vessels that supply oxygen to tumors.[12] Obviously, the size of the blood vessels that can be occluded in such a way depends on the PFP droplet size in the injected emulsion. In addition, for the passive targeting of hydrophobic drugs in PFP to tumors via the enhanced permeability and retention (EPR) mechanism, the PFP droplets must have the correct size range (10 − 100 nm) so that they pass only through the walls of blood vessels that supply tumors.[11] Thus, for both applications, the ability to control the mean PFP droplet size is of paramount importance. The interfacial tension value, as determined by the surfactants employed, is most likely an important determinant.

Figure 1a shows the chemical structure of PFP (C_5F_{12}, molecular weight 288 g/gmol), a member of the perfluorocarbon family. PFP is a liquid at room temperature but is a vapor at body temperature with a normal boiling point of 29.2 °C (Fluoromed, L. P. Product Information). At 25 °C, its density of 1.63 g/mL is much greater than that of water and its kinematic viscosity is much lower than that of water at 0.4 cSt.[13−15] As a result of its

*Corresponding author. E-mail: madhu.kandadai@utah.edu.

(1) Rogueda, P. G. A. HPFP, a Model Propellant for pMDIs. *Drug Dev. Ind. Phar.* **2003**, *29*, 39.
(2) Selvam, P.; Peguin, R. P. S.; Chokshi, U.; da Rocha, S. R. P. Surfactant design for the 1,1,1,2-tetrafluoroethane water interface: ab initio calculations and in situ high-pressure tensiometry. *Langmuir* **2006**, *22*, 8675−8683.
(3) Liu, Y.; Miyoshi, H.; Nakamura, M. Encapsulated ultrasound microbubbles: Therapeutic application in drug/gene delivery. *J. Controlled Release* **2006**, *114*, 89−99.
(4) Lowe, K. C. Fluorinated blood substitutes and oxygen carriers. *J. Fluorine Chem.* **2001**, *109*, 59−65.
(5) Harris, G. W.; Anderson, R. M.; Defilippi, R. P.; Nosé, Y.; Weber, D. C.; Malchesky, P. S. The physiological effects of fluorocarbon liquids in blood oxygenation. *J. Biomed. Mater. Res.* **1970**, *4*, 313−339.
(6) Porter, T. R.; Xie, F.; Kricsfeld, A.; Kilzer, K. Noninvasive identification of acute myocardial ischemia and reperfusion with contrast ultrasound using intravenous perfluoropropane-exposed sonicated dextrose albumin. *J. Am. Coll. Cardiol.* **1995**, *26*, 33−40.
(7) Gross, U.; Papke, G.; Rudiger, S. Fluorocarbons as blood substitutes: critical solution temperatures of some perflurocarbons and their mixtures. *J. Fluorine Chem.* **1993**, *61*, 11−16.
(8) Soman, N. R.; Lanza, G. M.; Heuser, J. M.; Schlesinger, P. H.; Wickline, S. A. Synthesis and characterization of stable fluorocarbon nanostructures as drug delivery vehicles for cytolytic peptides. *Nano Lett.* **2008**, *8*, 1131−1136.
(9) Krafft, M. P.; Riess, J. G. Perfluorocarbons: life sciences and biomedical uses *J. Polym. Sci., Part A: Polym. Chem.* **2007**, *45*, 1185−1198.
(10) Gerber, F.; Krafft, M. P.; Vandamme, T.; Goldmann, M.; Fontaine, P. Potential use of fluorocarbons in lung surfactant therapy. *Artif. Cells, Blood Substitutes, Biotechnol.* **2007**, *35*, 211−220.
(11) Rapoport, N.; Gao, Z.; Kennedy, A. Multifunctional nanoparticles for combining ultrasonic tumor imaging and targeted chemotherapy. *J. Natl. Cancer Inst.* **2007**, *99*, 1095−1106.
(12) Kripfgans, O. D.; Fowlkes, J. B.; Miller, D. L.; Eldevik, O. P.; Carson, P. L. Acoustic droplet vaporization for therapeutic and diagnostic applications. *Ultrasound Med. Biol.* **2000**, *26*, 1177−1189.
(13) Riley, T.; Stolnik, S.; Heald, C. R.; Xiong, C. D.; Garnett, M. C.; Illum, L.; Davis, S. S.; Purkiss, S. C.; Barlow, R. J.; Gellert, P. R. physicochemical evaluation of nanoparticles assembled from poly(lactic acid)-poly(ethylene glycol) (PLA-PEG) block copolymers as drug delivery vehicles. *Langmuir* **2001**, *17*, 3168.
(14) Pierri, E.; Avgoustakis, K. Poly(lactide)-poly(ethylene glycol) micelles as a carrier for griseofulvin. *J. Biomed. Mater. Res.* **2005**, *75A*, 639−647.
(15) Leyh, B.; Vangeyte, P.; Heinrich, M.; Auvray, L.; De Clercq, C.; Jérôme, R. Self-assembling of poly(ε-caprolactone)-b-poly(ethylene oxide) diblock copolymers in aqueous solution and at the silica-water interface. *Physica B: Condens. Matter* **2004**, *350*, E901−E904.

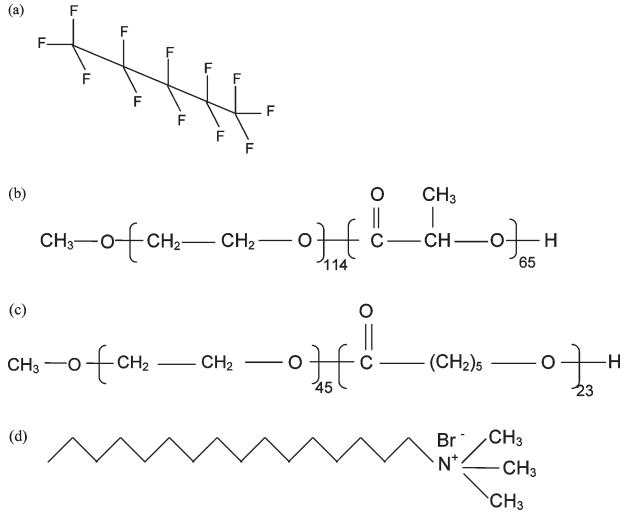

Figure 1. Chemical structures of (a) PFP, (b) PEO-PLA, (c) PEO-ε-PCL, and (d) CTAB.

nonpolar, hydrophobic nature, the solubility of oxygen in PFP at 25 °C (mole fraction 5.8×10^{-3}) is much higher than in water (mole fraction 2.3×10^{-5}) (Fluoromed, L. P. Product Information). PFP has also proven to be a nontoxic, noncarcinogenic biocompatible material.[5,7,10]

Because of the hydrophobic nature of PFP, it has a very high interfacial tension against water and does not readily disperse or dissolve in hydrophilic fluids. Hence, lowering the interfacial tension of PFP with surfactants is important to improving its dispersion in aqueous media. For the delivery of doxorubicin in PFP droplets to tumors, Rapoport et al.[11] used surfactants polyethylene oxide-*co*-polylactic acid (PEO-PLA, L form) and polyethylene oxide-*co*-poly-ε-caprolactone (PEO-PCL), which are uncharged block copolymers. The hydrophobic block (PLA or PCL) is thought to adsorb onto the PFP surface, and the hydrophilic PEO block is thought to form a "brush" that stabilizes the droplets against coalescence.

In contrast, cetyl trimethyl ammonium bromide (CTAB) is a well-known cationic surfactant with a relatively low molecular mass. The chemical structures of the surfactants are shown in Figure 1b−d. Above a certain concentration known as the critical micelle concentration (cmc), these surfactants form spherical core−shell-type micelles.[13] Typical cmc values for CTAB and BCP surfactants with similar molecular weights, from the literature, are shown in Table 1.

Bovine serum albumin (BSA) is a negatively charged globular protein and the most abundant protein in mammalian serum (4 wt % in human serum). It possesses a prolate ellipsoid tertiary structure with dimensions of $4 \times 4 \times 14$ nm. BSA has been shown to adsorb and denature at the air−water interface and reach an equilibrium surface tension of ∼53 dyn/cm.[38] Kripfgans et al. studied the PFP-BSA emulsion stability and droplet size distribution for occlusion therapy and ultrasound contrast applications.[12] They found that the PFP droplets in BSA solutions were stable against spontaneous vaporization at physiological temperature (37 °C) and ultrasonic scanning up to certain pressure thresholds and that their mean diameter and number density could be controlled by altering the concentration of BSA.

Table 1. Molecular Weights of the Surfactants Used in This Study and cmc Values from the Literature for CTAB and BCP Surfactants with Similar Molecular Weights

surfactant	molecular weight	PDI	literature cmc value in distilled water (mM)
$PEO_{114}-PLA_{65}$	9700	1.04	0.0071−0.0092[a]
$PEO_{45}-PCL_{23}$	4600	1.15	0.00014−0.0074[b]
CTAB	365	1.00	0.76−0.92[c]
BSA	66 000	1.00	0.000076[d]

[a] Reference 14. [b] References 15 and 16. [c] References 17−21. [d] Reference 22.

Because of their high molecular weights, BCP surfactants such as PEO-PLA and PEO-PCL possess a significantly lower cmc than smaller, nonpolymeric surfactant CTAB.[14−21]

The biocompatibility and biodegradability of PEO-PLA and PEO-PCL have been exploited in several biomedical applications such as bioresorbable sutures, orthopedic screws, coating materials, implants, and drug delivery.[14,23−33] Micelles formed by PEO-PLA and PEO-PCL are of particular interest because they can be used to sequester anticancer drugs, which are then delivered to tumors using PFP droplets.[11] CTAB, a cationic surfactant, has been used in several cosmetic products, topical antiseptic creams, and recently for the

(16) Lu, C.; Guo, S.; Liu, L.; Zhang, Y.; Li, Z.; Gu, J. Aggregation behavior of MPEG-PCL diblock copolymers in aqueous solutions and morphologies of the aggregates. *J. Polym. Sci., Part B: Polym. Phys.* **2006**, *44*, 3406−3417.

(17) Bergeron, V. Disjoining pressures and film stability of alkyltrimethylammonium bromide foam films. *Langmuir* **1997**, *13*, 3474−3482.

(18) Sepulveda, L.; Cortes, J. Ionization degrees and critical micelle concentrations of hexadecyltrimethylammonium and tetradecyltrimethylammonium micelles with different counterions. *J. Phys. Chem. B* **1985**, *89*, 5322−5324.

(19) Paredes, S.; Tribout, M.; Sepulveda, L. Enthalpies of micellization of the quaternary tetradecyl- and -cetyl ammonium salts. *J. Phys. Chem.* **1984**, *88*, 1871−1875.

(20) Cui, X.; Mao, S.; Liu, M.; Yuan, H.; Du, Y. Mechanism of surfactant micelle formation. *Langmuir* **2008**, *24*, 10771−10775.

(21) Bai, Y.; Xu, G.-Y.; Xin, X.; Sun, H.-Y.; Zhang, H.-X.; Hao, A.-Y.; Yang, X.-D.; Yao, L. Interaction between cetyltrimethylammonium bromide and cyclodextrin: surface tension and interfacial dilational viscoelasticity studies. *Colloid Polym. Sci.* **2008**, *286*, 1475−1484.

(22) Busscher, H. J.; van der Vegt, W.; Noordmans, J.; Schakenraad, J. M.; van der Mei, H. C. *Colloids Surf.* **1991**, 58.

(23) Allen, C.; Han, J.; Yu, Y.; Maysinger, D.; Eisenberg, A. Polycaprolactone-b-poly(ethylene oxide) copolymer micelles as a delivery vehicle for dihydrotestosterone. *J. Controlled Release* **2000**, *63*, 275−286.

(24) Hagan, S. A.; Coombes, A. G. A.; Garnett, M. C.; Dunn, S. E.; Davies, M. C.; Illum, L.; Davis, S. S.; Harding, S. E.; Purkiss, S.; Gellert, P. R. Polylactide-poly(ethylene glycol) copolymers as drug delivery systems. 1. characterization of water dispersible micelle-forming systems. *Langmuir* **1996**, *12*, 2153−2161.

(25) Hsu, S.-H.; Tang, C.-M.; Lin, C.-C. Biocompatibility of poly(ε-caprolactone)/poly(ethylene glycol) diblock copolymers with nanophase separation. *Biomaterials* **2004**, *25*, 5593−5601.

(26) Jongpaiboonkit, L.; Zhou, Z.; Ni, X.; Wang, Y.-Z.; Li, J. Self-association and micelle formation of biodegradable poly(ethylene glycol)-poly(L-lactic acid) amphiphilic di-block co-polymers. *J. Biomater. Sci., Polym. Ed.* **2006**, *17*, 747−763.

(27) Khor, H. L.; Ng, K. W.; Schantz, J. T.; Phan, T.-T.; Lim, T. C.; Teoh, S. H.; Hutmacher, D. W. Poly(ε-caprolactone) films as a potential substrate for tissue engineering an epidermal equivalent. *Mater. Sci. Eng., C* **2002**, *20*, 71−75.

(28) Liu, L.; Li, C.; Li, X.; Yuan, Z.; An, Y.; He, B. Biodegradable polylactide/poly(ethylene glycol)/polylactide triblock copolymer micelles as anticancer drug carriers. *J. Appl. Polym. Sci.* **2001**, *80*, 1976−1982.

(29) Li, Y.; Qi, X. R.; Maitani, Y.; Nagai, T. PEG-PLA diblock copolymer micelle-like nanoparticles as all-trans-retinoic acid carrier: in-vitro and in-vivo characterizations. *Nanotechnology* **2009**, *20*, 055106.

(30) Miura, H.; Onishi, H.; Sasatsu, M.; Machida, Y. Antitumor characteristics of methoxypolyethylene glycol-poly(dl-lactic acid) nanoparticles containing camptothecin. *J. Controlled Release* **2004**, *97*, 101−113.

(31) Serrano, M. C.; Pagani, R.; Vallet-Regí, M.; Peña, J.; Rámila, A.; Izquierdo, I.; Portolés, M. T. In vitro biocompatibility assessment of poly(ε-caprolactone) films using L929 mouse fibroblasts. *Biomaterials* **2004**, *25*, 5603−5611.

(32) Zhang, X.; Burt, H. M.; Hoff, D. V.; Dexter, D.; Mangold, G.; Degen, D.; Oktaba, A. M.; Hunter, W. L. An investigation of the antitumour activity and biodistribution of polymeric micellar paclitaxel. *Cancer Chemother. Pharmacol.* **1997**, *40*, 81−86.

(33) Zhong, Z.; Sun, X. S. Properties of soy protein isolate/polycaprolactone blends compatibilized by methylene diphenyl diisocyanate. *Polymer* **2001**, *42*, 6961−6969.

isolation of DNA from solutions containing other polysaccharides.[34,35]

No critical micelle concentration can be defined for BSA because it is not an amphiphilic surfactant. However, an apparent critical micelle concentration of ~0.076 μM is reported in the literature.[22] BSA has been studied as a potential emulsifier for PFP for occlusion therapy and ultrasound contrast enhancement.[12]

The interfacial behavior of hydrogenated or oxygenated fluoroalkanes in aqueous solutions containing low-molecular-weight surfactants, Pluronics,[1,2] and phospholipids[9,10,36,37] has been documented. However, the interfacial tension of perfluoropentane in aqueous solutions containing surfactants of any type has not, to our knowledge, been reported in the literature. Thus, the goal of this work is to compile and compare the interfacial tension of the PFP/water interface in the presence of the surfactants used in recent studies[11,12] to stabilize PFP emulsions for biomedical or pharmaceutical use.

Experimental Section

Materials. Research-grade PFP was purchased from Fluoromed L.P. and stored in a refrigerator at 0 °C in a sealed container. PEO_{114}-*b*-PLA_{65} diblock copolymer (Table 1) was purchased from Polymer Source Inc. (Canada) in a crystalline form. Because PEO-PLA crystals do not readily dissolve in water,[13] the aqueous solution of this BCP was prepared following a multistep process.[11] First, 0.125 g of the polymer was dissolved in 5 mL of THF with 20 mL of distilled water. Next, the organic solvent was removed by running the solution through a membrane tube with a molecular weight cutoff of 3500 Da (Spectra/Por, Spectrum Laboratories Inc., GA) followed by dialysis with water and 0.15 M Dulbecco's phosphate buffer solution (PBS). Distilled water was used to replace the volume of the organic solvent removed during the previous step to obtain the final 0.5% by weight PEO-PLA solution. The solution was allowed to homogenize by gentle agitation and was stored in a refrigerator when not in use. The solutions were diluted with 0.15 M PBS to obtain the desired concentrations. PEO_{45}-*b*-PCL_{23} diblock copolymer (Table 1) was also obtained from Polymer Source Inc. (Canada), and micellar solutions were prepared in a similar fashion.

Analytical-grade CTAB was purchased from Sigma. A 1 mM solution of CTAB in 0.15 M PBS was prepared and mixed by gentle agitation for 1 to 2 min and stored at room temperature.

Purified BSA (RIA and ELISA grade) was purchased from Calbiochem (San Diego, CA). Solutions were prepared in 0.15 M PBS, stored at ~0 °C, and used within 24 h of preparation.

Surface and Interfacial Tension Measurements. Gas-tight glass syringes (250 μL), flat-tipped stainless steel needles (14 gauge), and a two-way stainless steel valve were purchased from the Hamilton Company.

The syringe, needle, and valve were thoroughly cleaned before use and dried. The valve was used to control the flow of PFP from the syringe to the needle and control the size of the liquid drops. A glass environmental cell was cleaned thoroughly with distilled water and allowed to dry completely. For interfacial tension measurements, this cell was filled with surfactant solution.

The needle was then placed into the airtight glass cell as shown in Figure 2. For interfacial tension measurements, the needle tip

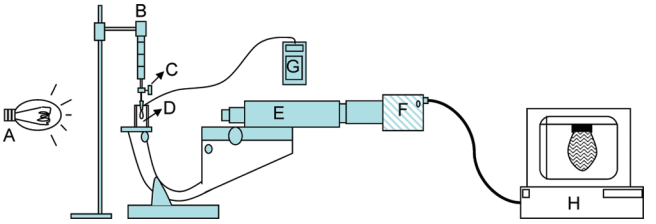

Figure 2. Experimental apparatus for surface/interfacial tension measurements. (A) Light source, (B) syringe, (C) two-way valve, (D) air-tight glass cell, (E) microscope, (F) CCD camera, (G) temperature monitor, and (H) computer.

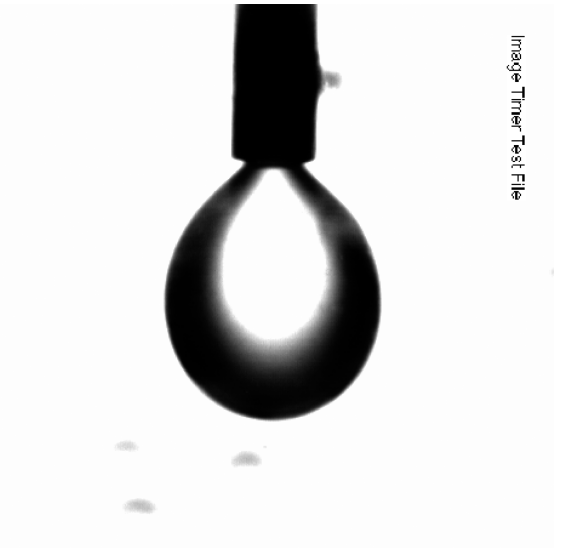

Figure 3. Image of a PFP drop in PEG-PLA surfactant solution captured by the CCD camera.

was submerged in surfactant solution and the temperature in the cell was constantly monitored using a wire thermocouple in direct contact with the solution.

All measurements were performed at room temperature (24 ± 1 °C).

PFP drops were injected into the surfactant solution, and images were captured using the CCD camera (Figure 3.). The first image was captured 5−10 s after the formation of the drop. The images were converted into pixel coordinates and then into coordinates in centimeters using Image 1.37 software.

The images were next analyzed using an axisymmetric drop shape analysis profile (ADSAP) program[38] that fits the drop coordinates to the Young−Laplace equation (Y−L equation) of capillarity.

The Y−L equation as described here is specifically for pendant drops and is derived by force balance over the suspended drop. This equation relates the pressure difference Δp across an interface between two fluids to the curvature of the interface, caused by the phenomenon of surface tension.

$$\Delta p = \gamma(1/R_1 + 1/R_2) \quad (1)$$

where γ is the surface/interfacial tension and R_1 and R_2 are the principle radii of curvature. The ADSAP program uses numerical integration to develop theoretical drop profiles to match the experimental drop profiles (Figure 4). The surface/interfacial tension, drop volume, drop surface area,

(34) Simões, M.; Pereira, M.; Machado, I.; Simões, L.; Vieira, M. Comparative antibacterial potential of selected aldehyde-based biocides and surfactants against planktonic Pseudomonas fluorescens. *J. Ind. Microbiol. Biotechnol.* **2006**, *33*, 741−749.

(35) Porebski, S.; Bailey, L.; Baum, B. Modification of a CTAB DNA extraction protocol for plants containing high polysaccharide and polyphenol components. *Plant Mol. Biol. Rep.* **1997**, *15*, 8−15.

(36) Bertilla, S. M.; Thomas, J.-L.; Marie, P.; Krafft, M. P. Cosurfactant effect of a semifluorinated alkane at a fluorocarbon/water interface: impact on the stabilization of fluorocarbon-in-water emulsions. *Langmuir* **2004**, *20*, 3920−3924.

(37) Burgess, D. J.; Yoon, J. K. Influence of interfacial properties on perfluorocarbon/aqueous emulsion stability. *Colloids Surf., B* **1995**, *4*, 297−308.

(38) Tripp, B. C.; Magda, J. J.; Andrade, J. D. Adsorption of globular proteins at the air/water interface as measured via dynamic surface tension: concentration dependence, mass-transfer considerations, and adsorption kinetics. *J. Colloid Interface Sci.* **1995**, *173*, 16−27.

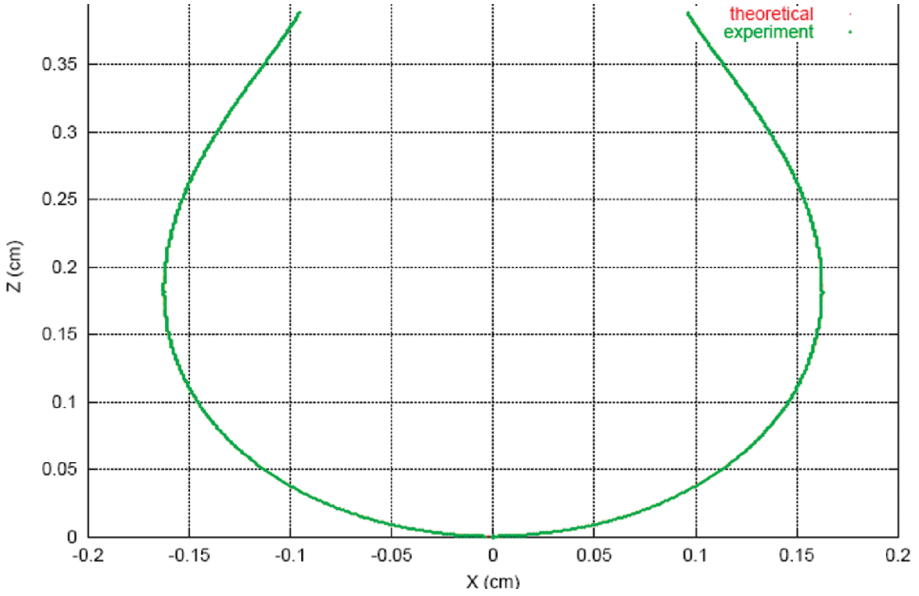

Figure 4. Comparison of the theoretical and experimental interface profile of a drop obtained through ADSAP.

Table 2. Literature and Experimental Values of the Equilibrium Surface Tensions of Surfactants at 25 °C Measured in This Study

material	concentration (mM)	solvent	equilibrium surface tension (dyn/cm)	literature value (in distilled water)	bond number
PFP (99% purity)			9.41	9.42[a]	0.42
CTAB	1	distilled water	29	35−38[b]	
		0.15 M PBS			
	1	0.15 M PBS	27		0.46
	0.4		27		0.41
PEO-PLA	0.15	0.15 M PBS	43	45−46[c]	0.41
	0.26		47		0.41
PEO-PCL	0.54	0.15 M PBS	47	49−52[d]	0.39
BSA	0.015	0.15 M PBS	43	53[e]	0.40

[a] References 48−51. [b] References 17 and 21. [c] References 41 and 52. [d] References 45 and 46. [e] References 38 and 47. The average standard deviation in the measured surface tension is 1 dyn/cm.

and radius of curvature of the drop were obtained by running the ADSAP program.

Results and Discussion

Bond Numbers. The Bond number (*Bo*) is a dimensionless group that represents the ratio between the gravitational force and surface/interfacial tension forces acting on a pendant drop[39,40] and is equal to

$$Bo = \Delta\rho g R_o^2/\gamma \quad (2)$$

where $\Delta\rho$ is the density difference at the surface or interface, g is the acceleration due to gravity, R_o is the radius of curvature of the drop at the apex, and γ is the surface or interfacial tension.

Spherical drops are obtained when this ratio is small.

In the presence of surfactants, the drop assumes a pendantlike ellipsoidal shape rather than a spherical shape because of the adsorption of molecules at the interface, resulting in a decrease in interfacial tension and an increase in the Bond number.

For an accurate pendant drop experiment, it is necessary that the drops have a pendantlike or ellipsoidal shape rather than a spherical shape. For spherical drops, the fit between the experimental and theoretical drop profile becomes independent of the surface/interfacial tension values.[38,39] This occurs when $Bo \ll 0.1$.

Bond numbers were calculated for the pendant drops for all of the systems studied. The average values are listed in Tables 2 and 3. For accurate results, the Bond number should lie between 0.1 and 0.6.[40] For all of our systems, the Bond numbers for the pendant drops were within this range.

The highest Bond numbers were obtained for systems involving CTAB surfactants, which were also the systems with the lowest surface/interfacial tension values.

Surface Tension of PFP at the Liquid/Air Interface. The surface tensions of PFP, distilled water, 0.15 M PBS, and various surfactant solutions were all measured against saturated air at room temperature. These measurements, which are not novel, are compared to values reported by previous authors as a check on our materials and experimental techniques. The measurements were repeatable with a low standard deviation (Table 2). Table 2 lists the measured equilibrium surface tension of the surfactant solutions (in PBS buffer) as well as literature values for solutions containing the same or similar (for the BCP) surfactants at their cmc's in distilled water. Our measured values are in reasonable agreement with literature values, with the possible exception of the BSA

(39) Tripp, B. C. Dynamic Surface Tension of Model Protein Solutions Measured via Pendant Drop Tensiometry. Ph.D. Dissertation, The University of Utah, Salt Lake City, UT, **1993**.

(40) Kim, J.-W.; Kim, H.; Lee, M.; Magda, J. J. Interfacial tension of a nematic liquid crystal/water interface with homeotropic surface alignment. *Langmuir* **2004**, *20*, 8110−8113.

(41) Tanodekaew, S.; Pannu, R.; Heatley, F.; Attwood, D.; Booth, C. Association and surface properties of diblock copolymers of ethylene oxide and DL-lactide in aqueous solution. *Macromol. Chem. Phys.* **1997**, *198*, 927−944.

Table 3. Interfacial Tensions of PFP against Water or 0.15 M PBS Containing Various Surfactants at the Concentrations Given

interface	surfactant	surfactant concentration (mM)	interfacial tension (dyn/cm) (±1−4 dyn/cm)	bond number
PFP-PBS			49	0.14
PFP-Water			54	0.15
			56[a]	
PFP-PBS	PEO-PLA	0.0103	38	0.17
		0.052	31	0.15
		0.103	29	0.17
		0.26	27	0.18
PFP-PBS	PEO-PCL	0.54	30	0.17
PFP-PBS	CTAB	0.05	17.7	0.42
		0.1	15.2	0.44
		0.2	12.6	0.46
		0.4	8.5	0.52
		0.6	10	0.48
		0.8	10.7	0.46
		1	10	0.58
PFP-PBS	BSA	0.015	31.1	0.58
		0.045	33.4	0.58
		0.075	28.0	0.52
		0.152	31.9	0.56
		0.227	30.8	0.56

[a] Reference 53.

solution. As reported previously,[39] the surface activity of proteins often varies with the supplier and also changes after repeated freeze−thaw cycles. The surface tension of distilled water (68 dyn/cm) was also found to be a little lower than the literature value of 72 dyn/cm, which we attribute to the accumulation of contaminants in water over the course of the experiment or fluctuations in room temperature. The lowest surface tension value is obtained using surfactant CTAB, which is unsurprising because it has the highest cmc value. As mentioned in Table 1, the literature values for the cmc's of PEO-PLA and PEO-PCL BCPs in aqueous solutions are very low.[14,15,24,26,29,41−46] CTAB, however, has a cmc value that is at least 2 orders of magnitude larger. Above the cmc, the surface tension becomes approximately independent of concentration, presumably because the concentration of unimers stays close to the cmc value and unimers are much more surface-active than micelles. Hence, even though our surfactant solution bulk concentrations were greater than the cmc value, the equilibrium surface tension values are nearly the same as the values reported at the cmc (Table 2). Similarly, for BSA, an apparent cmc of ∼0.076 μM has been reported in the literature,[22] with a constant equilibrium surface tension of 53−55 mN/m at higher concentrations.[38,47]

Interfacial Tension of PFP against Aqueous Solutions. In the absence of any surfactants, the interfacial tension of PFP against pure distilled water was measured to be 54 dyn/cm, in excellent agreement with the literature value of 56 dyn/cm.[53] Against 0.15 M PBS, the measured value was 49 dyn/cm. These very high values reflect the hydrophobicity of PFP, and hence surfactants are needed to disperse PFP in water.

In the presence of the block copolymer surfactants, the interfacial tension of PFP against water was measured in our laboratory to be about 27 dyn/cm for PEO-PLA and about 30 dyn/cm for PEO-PCL (Table 3). All concentrations studied were above the cmc of the block copolymers, which probably explains why no concentration dependence is observed in Figure 5.

In the presence of BSA, the interfacial tension of PFP against water was measured to be about 31 dyn/cm (Table 3) at all concentrations studied. In the presence of CTAB, a cationic surfactant, the interfacial tension of PFP against water reaches its lowest value, about 11 dyn/cm, at a concentration that is about one-half of the reported cmc value (Figure 5). As with the surface tension, the differing IFT behavior between CTAB on one hand and BSA, PEO-PLA, and PEO-PCL on the other hand can be explained by the much larger cmc value of CTAB. In all surfactant solutions, the unimer concentration should be close to the cmc value, and this is at least 2 orders of magnitude larger for CTAB than for the macromolecular surfactants. Thus, more surface-active species are available for adsorption onto the PFP surface when in contact with the CTAB solution. Given the very low cmc values of PEO-PLA and PEO-PCL, they are surprisingly effective in lowering the tension of the PFP/water interface. This suggests that the molecular size of the adsorbed species is also an important consideration. Globular BSA has dimensions of 4 nm × 4 nm × 14 nm,[54] spherical random coils of PEO-PLA have a hydrodynamic radius of about 35 nm,[13] and the fully extended CTAB tail has a length of 2.2 nm and a width of 0.3−0.5 nm.[55]

Significance to PFP Pharmaceutical Emulsion Preparation

Aqueous emulsions containing perfluorocarbons such as PFP,[11,12] perfluorobutane,[56] or decafluoropentane[57] that are suitable for biomedical applications such as occlusion and drug delivery

(42) Yang, L.; Zhao, Z.; Wei, J.; El Ghzaoui, A.; Li, S. Micelles formed by self-assembling of polylactide/poly(ethylene glycol) block copolymers in aqueous solutions. *J. Colloid Interface Sci.* **2007**, *314*, 470−477.
(43) Jiang, W.; Wang, Y.-D.; Gan, Q.; Zhang, J.-Z.; Zhao, X.-w.; Fei, W.-Y.; Bei, J.-Z.; Wang, S.-G. Preparation and characterization of copolymer micelles formed by poly(ethylene glycol)-polylactide block copolymers as novel drug carriers. *Chin. J. Process Eng.* **2006**, *6*, 289−295.
(44) Dai, Z.; Piao, L.; Zhang, X.; Deng, M.; Chen, X.; Jing, X. Probing the micellization of diblock and triblock copolymers of poly(l-lactide) and poly(ethylene glycol) in aqueous and NaCl salt solutions. *Colloid Polym. Sci.* **2004**, *282*, 343−350.
(45) Vangeyte, P.; Leyh, B.; Auvray, L.; Grandjean, J.; Misselyn-Bauduin, A. M.; Jerome, R. Mixed self-assembly of poly(ethylene oxide)-b-poly(ε-caprolactone) copolymers and sodium dodecyl sulfate in aqueous solution. *Langmuir* **2004**, *20*, 9019−9028.
(46) Vangeyte, P.; Leyh, B.; Heinrich, M.; Grandjean, J.; Bourgaux, C.; Jerome, R. Self-assembly of poly(ethylene oxide)-b-poly(ε-caprolactone) copolymers in aqueous solution. *Langmuir* **2004**, *20*, 8442−8451.
(47) McClellan, S. J.; Franses, E. I. Effect of concentration and denaturation on adsorption and surface tension of bovine serum albumin. *Colloids Surf., B* **2003**, *28*, 63−75.
(48) Freire, M. G.; Carvalho, P. J.; Queimada, A. J.; Marrucho, I. M.; Coutinho, J. A. P., Surface Tension of Liquid Fluorocompounds. *J. Chem. Eng. Data* **2006**, *51*, 1820−1824.
(49) Rohrback, G. H.; Cady, G. H. Surface tensions and refractive indices of the perfluoropentanes. *J. Am. Chem. Soc.* **1949**, 71.
(50) McLure, I. A.; Soares, V. A. M.; Edmonds, B. Surface tension of perfluoropropane, perfluoro-n-butane, perfluoro-n-hexane, perfluoro-octane, perfluorotributylamine and n-pentane. Application of the principle of corresponding states to the surface tension of perfluoroalkanes. *J. Chem. Soc., Faraday Trans. 1* **1982**, *78*, 2251−2257.
(51) Drummond, C. J.; Georgaklis, G.; Chan, D. Y. C. Fluorocarbons: surface free energies and van der Waals interaction. *Langmuir* **1996**, *12*, 2617−2621.
(52) Gref, R.; Babak, V.; Bouillot, P.; Lukina, I.; Bodorev, M.; Dellacherie, E. Interfacial and emulsion stabilising properties of amphiphilic water-soluble poly(ethylene glycol)−poly(lactic acid) copolymers for the fabrication of biocompatible nanoparticles. *Colloids Surf., A* **1998**, *143*, 413−420.
(53) Clasohm, L. Y.; Vakarelski, I. U.; Dagastine, R. R.; Chan, D. Y. C.; Stevens, G. W.; Grieser, F. Anomalous pH dependent stability behavior of surfactant-free nonpolar oil drops in aqueous electrolyte solutions. *Langmuir* **2007**, *23*, 9335−9340.
(54) Peters, T. *All about Albumin; Biochemistry, Genetics, and Medical Applications*; Academic Press: San Diego, CA, 1996.
(55) Palazzo, G.; Lopez, F.; Giustini, M.; Colafemmina, G.; Ceglie, A. Role of the cosurfactant in the CTAB/water/n-pentanol/n-hexane water-in-oil microemulsion. 1. Pentanol effect on the microstructure *J. Phys. Chem. B* **2003**, *107*, 1924−1931.
(56) Feshitan, J. A.; Chen, C. C.; Kwan, J. J.; Borden, M. A. Microbubble size isolation by differential centrifugation. *J. Colloid Interface Sci.* **2009**, *329*, 316−324.
(57) Huang, J.; Xu, J.; Xu, R. Heat-sensitive microbubbles for intraoperative assessment of cancer ablation margins. *Biomaterials* **2010**, *31*, 1278−1286.

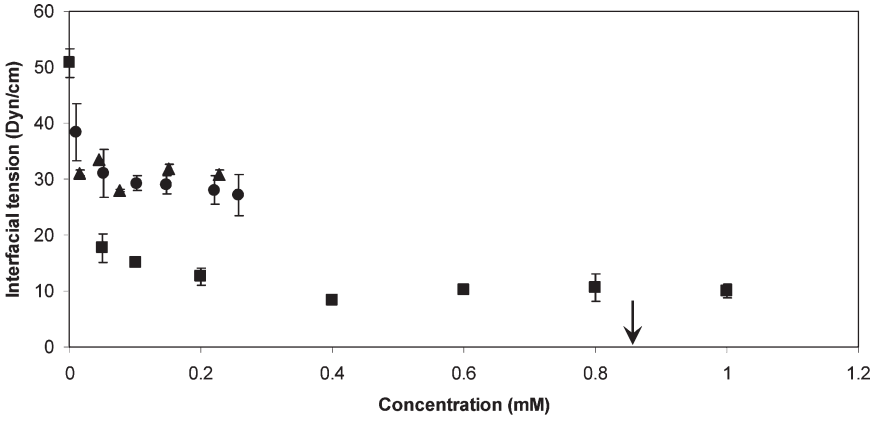

Figure 5. Interfacial tension between 0.15 M PBS and PFP as a function of bulk surfactant concentration at 24 °C. (●) PEO-PLA, (▲) BSA, and (■) CTAB. The vertical arrow gives the location of the literature cmc value for CTAB; the cmc values for BSA and PEO-PLA are both below 0.01 mM. Note that some error bars are not visible because they are smaller than or equal to the size of the symbols used because of very small standard deviations (< 1 dyn/cm).

have been prepared using surfactants PEO-PCL, PEO-PLA, BSA, and sodium cholate[11,12,57] without knowledge of the interfacial tension value. The results presented here show that all three of the macromolecular surfactants give similar values for the IFT value at high surfactant concentrations, approximately 30 dyn/cm. Perhaps this is the IFT value that produces the optimum drop size distribution (10−100 nm for EPR[11]), a proposition that we are checking by preparing PFP emulsions using CTAB as a surfactant. The results presented here also can be used to infer the minimum amount of surfactant that can be used to stabilize PFP emulsions. For example, Kripfagans et al. has reported using BSA concentrations of 0.015−0.24 mM (∼1−16 mg/mL).[12] The results in Figure 5 suggest that this is excessive because the IFT reaches its asymptotic value at a BSA concentration below 0.015 mM.

Conclusions

The very high interfacial tension value of PFP against water or PBS can be substantially lowered by all of the surfactants studied: BCP surfactants PEO-PLA and PEO-PCL, low-molecular-weight cationic surfactant CTAB, and anionic protein surfactant BSA. All of the macromolecular surfactants have been used previously to prepare stable PFP emulsions, whereas molecular-sized CTAB has not. All of the macromolecular surfactants give a similar value for the PFP/water tension (∼30 dyn/cm) that is independent of concentration, at least above very low reported cmc values. CTAB, which has a cmc value that is orders of magnitude larger, gives a limiting value for the tension of the PFP/water interface that is lower (10 dyn/cm). Given its low cmc value, PEO-PLA is surprisingly effective in lowering the tension of the PFP/water interface, probably because of its colloidal size. Furthermore, adsorption of the BCP likely gives rise to a PEO "brush" that stabilizes PFP droplets against coalescence or protein adsorption. The reduction in the surface tension of PBS buffer (against air) by PEO-PLA is also large. This may be relevant to biomedical applications in which the PFP liquid droplet is converted to a vapor within the body using ultrasound,[11] and the PFP vapor contains a significant mole fraction of oxygen because of the dissolution of oxygen from the surrounding aqueous solution into the PFP bubble.[58]

Acknowledgment. We thank Professor Natalya Rapoport for useful discussions. M.A.K., G.L., and J.J.M. acknowledge the donors of the American Chemical Society Petroleum Research Fund (grant 45968-AC9) and the National Institutes of Health (grant EB004947). P.M. and M.S. acknowledge support by the American Heart Association Established Investigator Award.

(58) Wustneck, N.; Wustneck, R.; Pison, U.; Mohwald, H. On the dissolution of vapors and gases. *Langmuir* **2006**, *23*, 1815−1823.